NJC

Cite this: *New J. Chem.*, 2011, **35**, 1701–1717

www.rsc.org/njc

PAPER

Synthesis of *N*-cyanoalkyl-functionalized imidazolium nitrate and dicyanamide ionic liquids with a comparison of their thermal properties for energetic applications†

David M. Drab,[a] Marcin Smiglak,[a] Julia L. Shamshina,[a] Steven P. Kelley,[a] Stefan Schneider,[b] Tommy W. Hawkins[b] and Robin D. Rogers*[a]

Received (in Gainesville, FL, USA) 10th November 2010, Accepted 20th April 2011
DOI: 10.1039/c0nj00889c

The synthesis of 10 *N*-alkyl-*N*-cyanoalkyl-functionalized imidazolium (*N*-methyl- and *N*-butyl-*N*-((CH_2)$_n$CN)imidazolium; n = 1–4) nitrate and 11 *N*-alkyl-*N*-cyanoalkyl-functionalized imidazolium (*N*-methyl-*N*-((CH_2)$_n$CN)imidazolium; n = 1–6, *N*-(2-cyanoethyl)-*N*-((CH_2)$_n$CN)imidazolium; n = 1,3–6) dicyanamide salts was achieved *via* *N*-alkylation of substituted imidazoles with commercially available haloalkylnitriles followed by anion exchange. Based on their observed melting points, all dicyanamide salts and all but one nitrate salt (1-cyanomethyl-3-methylimidazolium nitrate) had melting points <100 °C, as did 13 of the 17 halide precursors also reported here. Differential scanning calorimetry data indicated that melting points decreased by increasing the *N*-alkyl or *N*-cyanoalkyl chain length or by exchanging with the dicyanamide anion, which produced the lowest melting points in comparison to analogous halide or nitrate salts. Thermogravimetric analyses indicated that thermal stability increased for longer *N*-cyanoalkyl substituent lengths and decreased significantly for nitrates and more so for dicyanamides bearing short-chain *N*-cyanoalkyl substituents (*e.g.*, *N*-cyanomethyl, *N*-(1-cyanoethyl), and *N*-(2-cyanoethyl)) in comparison to halide precursors. Furthermore, for many of the *N*-cyanoalkyl-substituted salts (especially the dicyanamides), there was a significant production of thermally-stable char – presumably due to by-products formed from the reaction of either *N*-cyanoalkyl substituents, dicyanamide anion, or both, which resulted in thermally-stable polymers or cycles.

Introduction

There exists a high demand for the development of new and improved energetic materials (EMs) for application as propellants, fuels, and explosives, as traditional EMs face problems related to environmental and safety concerns during stages of synthesis, transport, and storage.[1] The U. S. Air Force, in particular, is interested in potential replacements of traditional energetic materials, and has recognized that ionic liquids (ILs, salts which have melting points <100 °C)[2] are valuable materials in energetic applications.[3,4] ILs often possess broad liquid ranges, negligible vapor pressures, high heats of formation, are thermally stable, and have significantly reduced sensitivity and toxicity characteristics. Additionally, their physical and chemical properties can be carefully tuned *via* the choice of the component ions to target specific performance properties.

As a result of the initial interest of the Air Force in energetic ionic liquids (EILs), intense research efforts have been made in this direction.[5–7] Promising results have appeared in the preparation of EILs with specific properties of interest to the Air Force – for example, high density,[8–11] high heats of formation,[12–14] optimal oxygen balance,[15–18] and hypergolicity.[19–23] However, there are not many strategies available to access these properties in a predictable manner.

Work in our group has been focused not on the synthesis of EMs *per se* but, rather, on the understanding of IL chemistry at a deeper level. It has long been an interest to identify IL structural patterns with the goal of accessing targeted properties in a systematic and predictable fashion. Previously, we have synthesized azole-based ILs with energetic substituents (*e.g.*, nitro-, amino-, cyano- groups) to identify the effect of azole type and ring substituents on thermal properties of resultant ILs.[24–26] In another study, we established a strategy to incorporate energetic functional groups into either cation or

[a] *Department of Chemistry and Center for Green Manufacturing, The University of Alabama, Tuscaloosa, AL 35487, USA. E-mail: rdrogers@as.ua.edu*
[b] *Air Force Research Laboratory, 10 East Saturn Boulevard, Building 8451, Edwards Air Force Base CA, USA. E-mail: Tommy.Hawkins@edwards.af.mil*

† CCDC reference numbers 801102–801105. For crystallographic data in CIF or other electronic format see DOI: 10.1039/c0nj00889c

anion, with the consequence that electron-withdrawing nitro- and cyano- groups were observed to deactivate azoles toward formation of cations.[13,19,27–29]

Continuing the above efforts, in this paper, we report systematic studies of thermal properties for two series of *N*-cyanoalkyl-functionalized imidazolium salts. Although there have been reported examples of *N*-cyanoalkyl-functionalized imidazolium halides,[30,31] nitrates,[32] and dicyanamides,[29,31,33] to the best of our knowledge these classes have not been examined systematically or comparatively with respect to homologous changes in structure.

Three types of systematic modifications to *N*-cyanoalkyl-functionalized imidazoliums have been made here. First, we believed that the length and branching of the alkyl chains in the *N*-cyanoalkyl-functionalized imidazolium cation would influence the liquid state, as others have reported melting point reduction as alkyl length increases.[34] We also hypothesized that the melting points of *N*-cyanoalkyl-functionalized imidazolium salts would be higher when compared with 1,3-dialkylimidazolium analogs, due to possible intra- and intermolecular organization from the π-electron system and lone pair electrons available in the cyano group.[26]

Secondly, for the same reason, we varied the *N*-alkyl substituent on the imidazole ring to probe for trends similar to those reported in the literature, where melting points typically decrease and thermal stabilities remain largely unaffected from *N*-methyl to *N*-butyl substitution.[34,35] Lastly, we investigated the effect of different energetic anions—nitrate and dicyanamide. Nitrate was chosen because of the oxidizing nature of the $[NO_3]^-$ anion, which facilitates thermal decomposition of the salt.[36] In turn, dicyanamide anions were expected to decrease melting points and increase thermal stability when compared to halide analogs.[37] In addition, the nitrate and dicyanamide anions were selected for their reputed IL-forming abilities and physicochemical properties suitable for EILs. These nitrile-functionalized salts are also excellent precursors to novel mixed heterocyclic species, as we have recently illustrated.[38]

Synthesis

The starting halide salts were obtained by alkylating commercially available methyl-, butyl-, or 2-cyanoethyl-substituted imidazole (Scheme 1: **1**, **2**, **3**, respectively)[39] with haloalkylnitriles *via* a classical quaternization reaction. Given the wide variety of commercially available haloalkylnitriles, this was considered a logical starting point for the synthesis of imidazolium salts with variable *N*-cyanoalkyl side-chain lengths as described here.[40] The *N*-cyanoalkyl-functionalized imidazolium nitrate (**4–7**, **10-15[NO_3]**), and dicyanamide (**4–9**, **16-20[$N(CN)_2$]**) salts were prepared by metathesis of the analogous halides (**4-20[X]**), either by using an ion exchange resin (nitrate salts) or a silver salt (dicyanamide salts).

The 17 *N*-cyanoalkyl-functionalized imidazolium halide salts (**4-20[X]**) were synthesized according to literature protocols,[41,42] where 1-alkylimidazole starting materials (**1–3**) were alkylated with haloalkylnitriles generally under solvent-free conditions at 70 °C for 48 h in a sealed, high-pressure vial (except as noted below). Since the main focus of the work was to investigate how the properties of the nitrate and dicyanamide salts are affected by changing the *N*-cyanoalkyl substituent, the uniformity of the halide anion in the synthesis of **4-20[X]** was not considered essential and was established by the availability of commercial haloalkylnitriles.

Minor changes were implemented in the published reactions. The syntheses of **4[Cl]**, **11[Cl]**, and **16[Cl]** were conducted at room temperature to avoid the thermal degradation of the substrates. In addition, **8[Br]**, **9[Br]**, and **17-20[X]** were all prepared using ethyl acetate as solvent to allow for easy product phase separation from the solvent layer. Upon washing **4-20[X]** with ethyl acetate or acetone, and subsequent removal of residual solvent under high vacuum overnight, the halide salts were obtained in fair to excellent yields (82–97%) with the exception of **11[Cl]** (yield = 57%) and **14[Cl]** (yield = 45%, as a result of inadvertent loss of sample when removing residual starting materials).

Many of the intermediate halide salts have been synthesized previously including, **4[Cl]**,[30,42] **5[Br]**,[43] **6[Cl]**,[30] **7[Cl]**,[30] **12[Br]**,[44] and **16[Cl]**.[38] Since these compounds were typically only used as intermediates in further IL synthesis, important data such as melting points, glass transition temperatures, thermal stability, and synthetic yields were frequently not reported. Here, we report all of the thermal properties and yields for these intermediates and, where possible, compare them with the literature. To the best of our knowledge, the nitrate (**4–7**, **10-15[NO_3]**) and dicyanamide (**4**, **5**, **7–9**, **16-20[$N(CN)_2$]**) salts were not previously reported, with the exception of **6[$N(CN)_2$]**.[31]

Nitrate salts **4–7**, **10-15[NO_3]** were prepared from the halide precursors using the strongly basic anion exchange resin BioRad AG 1-X8 (100–200 mesh with 8% divinylbenzene copolymer cross-linkage). The resin has an exchange capacity of 2.6 meq/g dry resin and an appropriate amount of resin was prepared to exchange 3.2 to 6.4 mmol of halide precursor. The commercially available chloride resin was converted to $(NO_3)^-$-form following the manufacturer's protocol,[45,46] where the resin was loaded into a column (1 cm diameter × 10 cm tall) and washed with 5 bed volumes of 0.5 N sodium nitrate solution. To check for the completeness of the nitrate exchange, the presence of halide in the eluted solution was spot checked frequently with a 1.0 M silver nitrate solution. When no halide was indicated as evident by the lack of white, cloudy precipitate, final conditioning of the nitrate-exchanged resin column was completed by washing with 2 bed volumes of deionized water.

With the (NO_3^-)-form of the resin in hand, halide samples were dissolved in 100 mL of deionized water and eluted through the column followed by an additional 2 bed volumes of deionized water in the final rinse. For both nitrate loading and sample elution, the linear flow rate was maintained at approximately 2 cm min^{-1} through the bed volume. Each of the eluted fractions was qualitatively screened for the presence of halide by spot-testing each eluted fraction with 1.0 M silver nitrate solution. Once separated, the 'halide-free' fractions were then purified by removal of water from the nitrate salts using an air stream followed by final drying under high vacuum for 24 h. The final 10 products **4–7**, **10-15[NO_3]** were obtained in fair to excellent yields (76–95%).

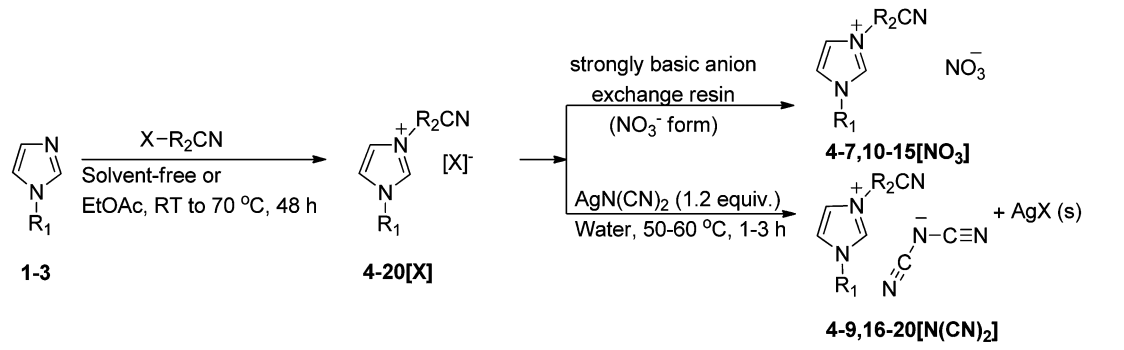

1: R_1 = methyl (Me)
2: R_1 = butyl (Bu)
3: R_1 = 2-cyanoethyl ($(CH_2)_2CN$)

4: R_1 = Me, R_2 = CH_2
5: R_1 = Me, R_2 = $(CH_2)_2$
6: R_1 = Me, R_2 = $(CH_2)_3$
7: R_1 = Me, R_2 = $(CH_2)_4$
8: R_1 = Me, R_2 = $(CH_2)_5$
9: R_1 = Me, R_2 = $(CH_2)_6$
10: R_1 = Me, R_2 = $CH(CH_3)$

11: R_1 = Bu, R_2 = CH_2
12: R_1 = Bu, R_2 = $(CH_2)_2$
13: R_1 = Bu, R_2 = $(CH_2)_3$
14: R_1 = Bu, R_2 = $(CH_2)_4$
15: R_1 = Bu, R_2 = $CH(CH_3)$

16: R_1 = $(CH_2)_2CN$, R_2 = CH_2
17: R_1 = $(CH_2)_2CN$, R_2 = $(CH_2)_3$
18: R_1 = $(CH_2)_2CN$, R_2 = $(CH_2)_4$
19: R_1 = $(CH_2)_2CN$, R_2 = $(CH_2)_5$
20: R_1 = $(CH_2)_2CN$, R_2 = $(CH_2)_6$

Scheme 1 Synthesized *N*-cyanoalkyl-functionalized imidazolium halide (**4-20[X]**), nitrate (**4–7**, **10-15[NO_3]**), and dicyanamide (**4–9**, **16-20[$N(CN)_2$]**) salts.

The dicyanamide salts **4–9**, **16-20[$N(CN)_2$]** were obtained by metathesis using silver dicyanamide (prior attempts to obtain dicyanamide salts using sodium dicyanamide by literature protocols failed to achieve satisfactory yields[47]) which was prepared by methods reported in the literature.[19,33] Each of the halide precursors (**4–9**, **16-20[X]**) was combined with a 10% excess of $AgN(CN)_2$ in deionized water and heated at 50 °C for 1 h. At the end of the metathesis reaction, the silver halide by-product was filtered, and subsequent evaporation of water from the filtrate using an air stream resulted in the 11 dicyanamide salts in fair to good yields (75–92%). One of these compounds, **6[$N(CN)_2$]**, has been previously reported,[31] and the published data is discussed below in the comparison of all compounds.

To check purity at each stage of the synthesis, ^{1}H NMR analysis confirmed the structure of all cations (**4–20**) and served as a check for the presence of organic starting materials in **4–7**, **10-15[NO_3]** and **4–9**, **16-20[$N(CN)_2$]**, which were found to be below detection limits (<1 mol%).[48] FT-IR spectroscopy was used to identify the characteristic intense absorption band for the free nitrate anion (ν_{max}(N–O) = 1350–1360 cm^{-1})[49] in **4–7**, **10-15[NO_3]**, as well as those observed for the dicyanamide anion (ν_{max}(C≡N) region around 2250 (m), 2220 (m), and 2150 (s) cm^{-1}).[50] Spot-testing the eluted nitrate salt fractions with silver nitrate solution served to qualitatively confirm the absence of halide in the final product with the complete anion exchange of halide for nitrate (<100 ppm).[51] Determination of halide impurity in the dicyanamide samples was attempted following a literature method[52,53] that used silver nitrate titration in the presence of a potassium chromate indicator, however, this did not conclusively indicate halide in the samples obtained.

Single crystal structures by X-ray diffraction

Crystallographic analyses were performed on the halide salts **5[Br]** and **10[Br]**, the nitrate salt **4[NO_3]**, and the dicyanamide salt **4[$N(CN)_2$]**. Single crystals were obtained by recrystallization from methanol solutions with slow-vapor diffusion using diethyl ether. The crystallographic details can be found in the Electronic Supplementary Information (ESI).†

The asymmetric units for each of the solved structures are shown in Fig. 1, where each structure is oriented perpendicular with respect to the plane of the imidazolium ring. The bond lengths and angles are all typical for the imidazolium ring, although the bonds involving C2 in **4[$N(CN)_2$]** (Fig. 1D) are significantly shorter than the others, and there is variability of the C–CN bond among the structures. All imidazolium rings are fairly planar, although **10[Br]** (Fig. 1B) has the least planar ring.

The overall packing in **5[Br]** is salt-like (Fig. 1A), but the nitrile groups do not participate in short contacts. Crystal structures of 1-(2-cyanoethyl)-3-methylimidazolium salts have not yet been reported in the literature, but in three similar salts, the nitrile groups participate in a variety of close contacts with the cation such as parallel 'stacking' with the imidazolium ring,[30] contacts with other parallel nitrile groups, and contacts to hydrogen atoms on the cation.[54] Nitrile-imidazolium short contacts are observed in the other 3 structures reported here (Fig. 1B, C and D), and together these observations imply that it is unusual that the nitrile groups in **5[Br]** do not participate in short contacts. The cations do interact *via* edge-to-edge π–π stacking between the C4 and C5 positions (C4···C5 = 3.413(2) Å). The anions interact through hydrogen bonds to hydrogen atoms at the C2 and C4 positions, but do not appear to reside in the coloumbically favorable positions above and below the imidazolium ring.[19]

10[Br] also shows salt-like packing with alternating anion and cation layers. There are short contacts between cations involving the nitrile group and hydrogen atoms, as well as pi-stacked cation dimers with C4 on one ring approaching C5 on another at a distance of 3.559(3) Å, with the rings parallel. The anions participate in three different interactions with

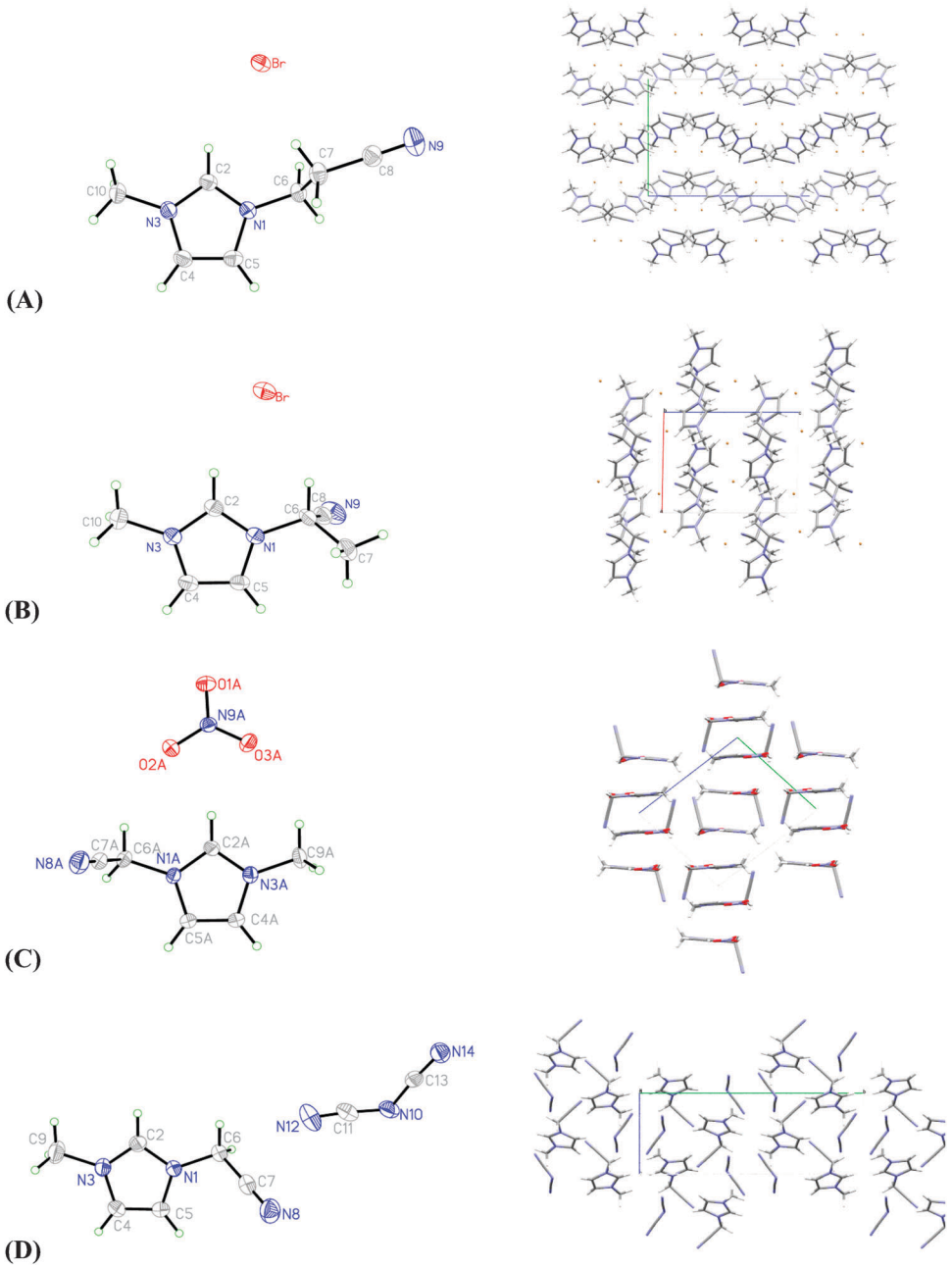

Fig. 1 ORTEP illustrations (50% probability ellipsoids) of the formula units (illustrating the closest cation–anion approach) and packing diagrams for **5[Br]** down *c* (A), **10[Br]** down *a* (B), **4[NO_3]** down *a* (C) , and **4[$N(CN)_2$]** down *a* (D). Crystallographic axes are color-coded: *a* is red, *b* is green, and *c* is blue.

cations: a hydrogen bond to the hydrogen at the C2 position, a hydrogen bond to a hydrogen atom at the C5 position, and an out-of-plane interaction with the C2 carbon atom from one side of the ring.

4[NO_3] has two symmetry-independent formula units, however, the environment and packing is the same for both of them. Packing seems to be dominated by cation–anion interactions with the side-chains oriented to maximize hydrogen bonding to the nitrile group, where all anions and imidazolium rings are roughly parallel. Cation-cation short contacts occur between the hydrogen atom at C4 and nitrile groups on two cations (a bifurcated contact). The anion makes three in-plane hydrogen bonds: a very short, bifurcated contact between the oxygen atoms and the hydrogen atom on C2, a bifurcated hydrogen bond to the hydrogen atom at C5, and short contacts to the methylene hydrogen atoms and C7. There is also an out-of-plane interaction between the anion and C2.

4[$N(CN)_2$] also shows efficient salt-like packing with separate anion and cation layers. This structure has only one cation–cation short contact, which is between the nitrile group and the methylene hydrogen atoms. The anion exhibits several types of interactions, with each atom participating differently. One of the terminal nitrogen atoms, N14, makes a hydrogen bond to H2A on one cation, a short contact to the methyl

group on a second cation, and is situated above the C2 position of a third cation. N10 makes a hydrogen bond to a ring hydrogen atom at C5. C11 makes short contacts to a methyl group on one cation and C2 on another cation. The carbon atoms in the dicyanamide anion behave as hydrogen bond acceptors as was reported for other related crystal structures.[19,50,55]

Thermal and sensitivity investigations

Most of the 41 compounds synthesized and reported here are ILs by definition (*i.e.*, mp <100 °C), with the exception of **4[Cl]**, **5[Br]**, **6[Cl]**, **4[NO_3]**, **5[NO_3]**, and **4[$N(CN)_2$]** which are all crystalline solids. Phase transition temperatures were obtained by DSC (Table 1) and include crystallization and melting transition temperatures (T_{cryst} and T_m, respectively), as well as glass and liquid–liquid transition temperatures (T_g and T_{l-l}, respectively). T_g and T_{l-l} were determined from the second heating cycle after initially heating the material from ambient temperature to an upper limit based upon the thermal stability of the compound as determined by TGA. Phase transitions determined after the first heating cycle were considered to be generally more accurate, where there is evidence for improved surface contact between the sample and the DSC sample pan in subsequent heating cycles.[56]

We have observed liquid–liquid transitions for ILs fairly often, particularly in our work with pharmaceutical ionic liquids.[57] The recent work of Tanaka *et al.*[58,59] suggests our observed results are indicative of differing liquid states and that such transitions are expected to be common for ionic liquids.

Crystallization was taken as the onset for an exothermic peak in the second heating cycle (with the exception of **4[NO_3]**, which showed T_{cryst} = 43 °C as an exothermic peak during each cooling cycle) and these are typical for transformations of super-cooled liquids to crystalline solids.[60] T_m values were measured from the onset of a sharp, endothermic peak on heating, and T_g values were identified from the onset of small shifts in heat flow arising from the transition between amorphous glassy to liquid states when heating.

The thermal stabilities (by TGA) for all prepared compounds are presented in Table 1 as the onset of thermal decomposition for the first 5% weight loss ($T_{5\%onset}$). The value for $T_{5\%onset}$ was considered a more accurate assessment of thermal stability than the onset of thermal decomposition (T_{onset}, included for comparison in parentheses in Table 1) that is more commonly reported in the literature.[61] All compounds were heated to 600 °C at a rate of 5 °C min^{-1} with an isothermal hold at 75 °C for 30 min.

Sensitivity testing for all dicyanamide salts **4–9**, **16-20[$N(CN)_2$]** was conducted using an Olin-Mathieson drop weight tester, and the values obtained are reported in the last column of Table 1. In addition, the same compounds were tested for sensitivity to friction using a Julius Peters apparatus, as well as sensitivity to electrostatic discharge (ESD) using an Air Force Research Laboratory ESD test apparatus with initial sample test level at 5000 V with capacitance set to deliver 0.25 J.

Differential scanning calorimetry

The observed thermal behavior of the *N*-cyanoalkyl-functionalized salts was often complex, and phase transitions were classified according to one of four different observations. Fig. 2 compares the first and second heating cycles were for representative compounds **16[$N(CN)_2$]**, Class I; **6[Cl]**, Class II; **12[Br]**, Class III; and **4[NO_3]**, Class IV.

The most common trend in the DSC data (Fig. 2, Class I) featured a reversible glass transition followed by an additional liquid–liquid transition during the second and third consecutive heating cycles. Compounds of this type include **7[Cl]**, **8[Br]**, **9[Br]**, **11[Cl]**, **13[Cl]**, **14[Cl]**, **15[Br]**, **17[Cl]**, **18[Cl]**, **19[Br]**, **20[Br]**; **6**, **7**, **11-15[NO_3]**; and **5–9**, **16-20[$N(CN)_2$]**. Structural features common to this class include the *N*-butyl-substituted nitrate salts, most of the dicyanamide ILs (Class II **4[$N(CN)_2$]** is an exception), and the halide salts featuring longer *N*-cyanoalkyl functional groups.

Those compounds in Class II did not show melting on the first heating cycle but, rather, featured a reversible, low-temperature glass transition, crystallization on heating from a super-cooled phase, and a subsequent melting transition. This class of thermal behavior was observed for compounds **4[Cl]**, **6[Cl]**, **10[Br]**, **5[NO_3]**, **10[NO_3]**, and **4[$N(CN)_2$]** (Fig. 2, Class II), which featured short *N*-cyanoalkyl chain lengths (*e.g.*, *N*-cyanomethyl, *N*-(1-cyanoethyl), and *N*-(2-cyanoethyl)), with the exception of **6[Cl]** that was functionalized with the *N*-(3-cyanopropyl) group.

There were also a few examples for which the thermal behavior differed significantly from the above. For example, in three cases melting occurred in the first heating cycle but only a reversible glass transition prior to a liquid–liquid transition was observed for the next consecutive heating cycles. This small class of compounds consists of all halide salts featuring the *N*-(2-cyanoethyl) functional group (Fig. 2, Class III, compounds **5[Br]** **12[Br]**, and **16[Cl]**).

Finally, in a single case melting was observed for each heating cycle, as well as crystallization for each cooling cycle (Fig. 2, Class IV, **4[NO_3]**). For this compound, there was no glass transition observed. The melting point for **4[NO_3]** (T_m = 103 °C) was the highest observed for all nitrates and dicyanamide salts, presumably from the more efficient packing of the smallest cation (**4**) of the nitrate salt. However, several halides with short *N*-cyanoalkyl groups were observed to have significantly higher melting points (T_m = 174 °C, **4[Cl]**; 143 °C, **5[Br]**; 131 °C, **10[Br]**, 120 °C, **16[Cl]**), which results from the small size of both cation and anion.

Class I compounds did not exhibit well-defined melting temperatures, which is consistent with the suggestion that the relatively high viscosity of ILs (compared to molecular liquids) can inhibit crystallization during the timeframe of the DSC experiment.[62] Our group has observed similar thermal behavior previously for a series of protonated ILs,[63] and it was proposed that the varying degree of inclination in the onset of the T_{l-l} signal might indicate variation of crystallization attempts for the ILs. Fig. 3 compares the second heating cycles for four of the Class I compounds, where the variation in slope of the T_{l-l} onset varies significantly in both the exothermic rise as well as the endothermic trough.

Table 1 Thermal and sensitivity characterization of halide, nitrate, and dicyanamide salts with cations **4–20**

			$[X]^-$				$[NO_3]^-$			$[N(CN)_2]^-$			
Cation	Cation#	R_2CN	[X]	T_g (T_{l-l}) (°C)[a]	T_m (T_{cryst}) (°C)[a]	$T_{5\%onset}$ (T_{onset}) (°C)[b]	T_g (T_{l-l}) (°C)	T_m (T_{cryst}) (°C)	$T_{5\%onset}$ (T_{onset}) (°C)	T_g (T_{l-l}) (°C)	T_m (T_{cryst}) (°C)	$T_{5\%onset}$ (T_{onset}) (°C)	Impact (kg cm)[c]
	4	CH_2CN	Cl^-	36	174 Lit. 170[34] (114)	206 (251) (Lit. 221[38])	—	103 (43)	183 (195)	**−60**	**67** (12)	210 (234)	>200
	5	$(CH_2)_2CN$	Br^-	−21	143	205 (241)	**−47**	**62** (1.9)	166 (198)	**−67**	**12**	161 (173)	172
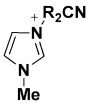	6	$(CH_2)_3CN$	Cl^-	**−35** Lit. −34[30]	**96** Lit. 90[30] **(21)** (Lit. 26[30])	258 (290) (Lit. T_d = 255[30])	**−56** **(38)**	—	223 (270)	**−80** Lit. −72[31] **(50)**	—	244 (260) (Lit. T_d = 278[31])	170
	7	$(CH_2)_4CN$	Cl^-	**−51** **(45)**	Lit. 32[30]	224 (262)	**−56** **(52)**	—	266 (294)	**−74** **(47)**	—	247 (273)	170
	8	$(CH_2)_5CN$	Br^-	**−44** **(50)**	—	248 (284)	n.s.	n.s.	n.s.	**−78** **(59)**	—	264 (287)	170
	9	$(CH_2)_6CN$	Br^-	**−48** **(49)**	—	257 (280)	n.s.	n.s.	n.s.	**−77** **(46)**	—	266 (289)	170
	10	$CH(CH_3)CN$	Br^-	−3.1	131 (76)	219 (254)	**−58**	**42** **(−9.7)**	168 (209)	n.s.	n.s.	n.s.	n.s.
	11	CH_2CN	Cl^-	**−22** **(114)**	—	186 (213)	**−43** **(46)**	—	168 (179)	n.s.	n.s.	n.s.	n.s.
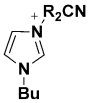	12	$(CH_2)_2CN$	Br^-	**−31** **(52)**	**86**	227 (259)	**−52** **(63)**	—	180 (202)	n.s.	n.s.	n.s.	n.s.
	13	$(CH_2)_3CN$	Cl^-	**−36** **(40)**	—	243 (279)	**−59** **(48)**	—	258 (292)	n.s.	n.s.	n.s.	n.s.
	14	$(CH_2)_4CN$	Cl^-	**−39** **(50)**	—	240 (278)	**−59** **(42)**	—	263 (291)	n.s.	n.s.	n.s.	n.s.
	15	$CH(CH_3)CN$	Br^-	**−12** **(132)**		211 (246)	**−50** (50)	—	157 (214)	n.s.	n.s.	n.s.	n.s.
	16	CH_2CN	Cl^-	0.26 (49)	120	196 (222)	n.s.	n.s.	n.s.	**−43** **(50)**	—	148 (162)	176
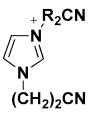	17	$(CH_2)_3CN$	Cl^-	**−27** **(95)**	—	196 (210)	n.s.	n.s.	n.s.	**−62** **(72)**	—	164 (182)	176
	18	$(CH_2)_4CN$	Cl^-	**−36** **(51)**	—	190 (221)	n.s.	n.s.	n.s.	**−61** **(51)**	—	170 (178)	174
	19	$(CH_2)_5CN$	Br^-	**−42** **(52)**	—	202 (241)	n.s.	n.s.	n.s.	**−66** **(53)**	—	165 (192)	174
	20	$(CH_2)_6CN$	Br^-	**−42** **(58)**	—	161 (221)	n.s.	n.s.	n.s.	**−66** **(58)**	—	157 (192)	170

[a] Melting point (T_m) and/or glass transition temperatures (T_g) were measured from the onset of transition and determined by DSC from the second heating cycle at a ramp rate of 5 °C min^{-1} after initially melting then cooling the samples to −100 °C, unless otherwise indicated. Salts meeting the definition of ionic liquids (mp <100 °C) are in **bold**. [b] Reported decomposition temperatures were obtained by TGA, heating at 5 °C min^{-1} under dried air atmosphere and are reported as (i) onset to 5 weight% loss of mass ($T_{5\%onset}$) and (ii) onset to total mass loss (T_{onset}) (in parentheses). [c] Impact sensitivity analysis was carried out on an Olin-Mathieson drop weight tester where a small sample (20 mg) was placed in a standard sample cup (liquid or solid cell employed as appropriate), and a multi-kilogram mass was dropped vertically from measured heights upon the closed sample. [d] n.s. = not synthesized.

For the example **5[N(CN)$_2$]** (Fig. 3A), the observed sharp exothermic increase might signify the start of crystallization. However, the plateau of the signal maxima and broad endothermic trough are not characteristic of typical crystallization/melt curves as found, for example, in Class II compounds. The other compounds shown in Fig. 3 also indicated increasingly glass-like transitions from a super-cooled phase (compare Fig. 3B–C), where changing heat flow both in the onset and offset of the signal differed from the characteristic shift of glass transitions. Further DSC study of these materials at slower DSC scan rates may provide a greater understanding of this complex thermal behavior, where others have interpreted similar thermal behavior as a result of conformational disorder,[56,64,65] or plastic crystalline behavior as extensively reported by MacFarlane and co-workers.[66–69]

Without exception, the T_g for salts of the same cation structure decreased in the order of $[X]^-$ > $[NO_3]^-$ > $[N(CN)_2]^-$. In addition, compounds that showed melting behavior also followed this trend (*N*-cyanomethyl-functionalized: T_m = 174 °C, **4[Cl]**; 103 °C, **4[NO$_3$]**; 67 °C, **4[N(CN)$_2$]**; *N*-(2-cyanoethyl)-functionalized: T_m = 143 °C, **5[Br]**; 62 °C, **5[NO$_3$]**; 12 °C, **5[N(CN)$_2$]**). Increasing proton affinity and

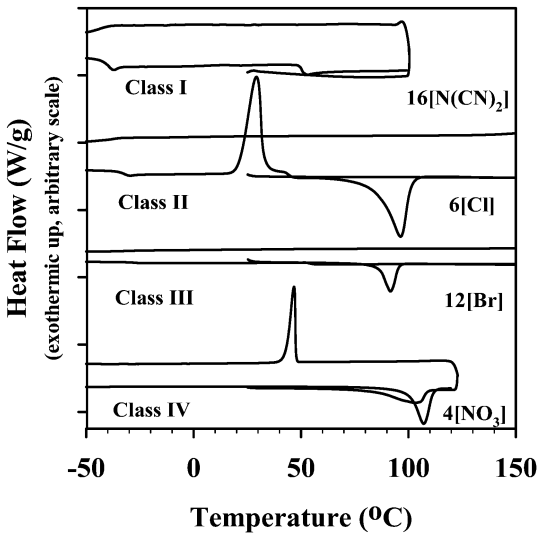

Fig. 2 Comparison of first and second heating cycle DSC data exemplifying different classes of thermal behavior: **16[N(CN)$_2$]** (Class I), **6[Cl]** (Class II), **12[Br]** (Class III), and **4[NO$_3$]** (Class IV).

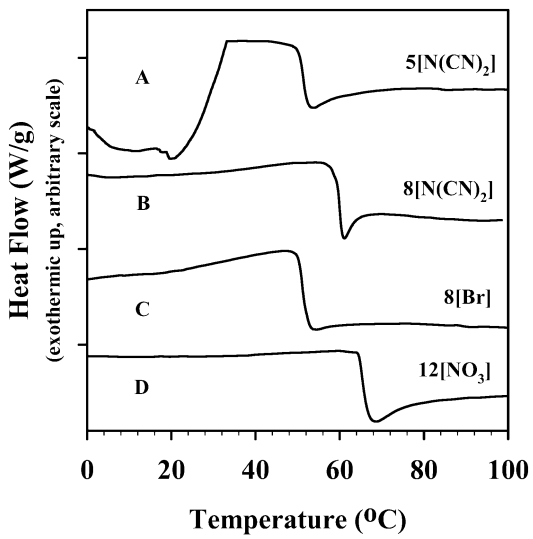

Fig. 3 Selected DSC traces showing varying degrees of curvature in T_{l-l} transition from a super-cooled liquid state on the second heating cycle.

diffusivity of the negative charge in the anion, in part, may explain the lower T_g observed for nitrate and dicyanamide salts, respectively.[70,71] These factors can also affect the hydrogen-bonding interactions of the anion and, thus, influence the molecular packing and the observed melting points for the compounds.[72] Other factors such as differences in the anion size ($[X]^- < [NO_3]^- < [N(CN)_2]^-$) have also been found to correlate with decreasing melting points in ILs.[73]

Shorter *N*-cyanoalkyl-substituted halide salts with the *N*-methyl group showed high temperature melting transitions (T_m = 174 °C, **4[Cl]**; 143 °C, **5[Br]**, 96 °C, **6[Cl]**), whereas only one case of an *N*-butyl-substituted halide salt was found to have a melting transition (T_m = 86 °C, **12[Br]**). This behavior has been attributed to the less efficient packing of ions for longer *N*-alkyl and *N*-cyanoalkyl substituents, resulting in

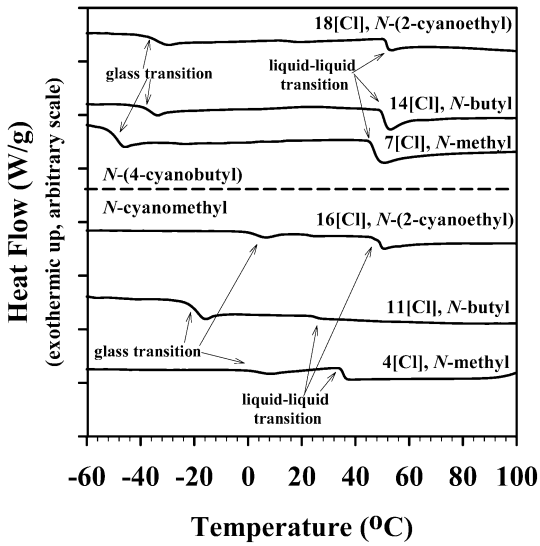

Fig. 4 Comparison of glass transition (T_g) and liquid–liquid transition (T_{l-l}) trends in DSC data for *N*-cyanomethyl- (bottom) and *N*-(4-cyanobutyl)-functionalized (top) chloride salts with different *N*-alkyl substituents (*N*-methyl, *N*-butyl, and *N*-(2-cyanoethyl)).

liquid-state properties at lower temperatures.[37] In Fig. 4, the observed trends in thermal behavior with changing *N*-cyanoalkyl and *N*-alkyl substituent lengths are illustrated for a selection of the chloride salts reported here.

A higher T_g was observed for *N*-methyl-substituted **4[Cl]** compared to analogous *N*-butyl **11[Cl]** (Fig. 4, bottom), where less efficient packing of *N*-butyl- *vs.* *N*-methyl-substituted cations has been reported to promote the liquid state at lower temperatures.[2] Higher T_g values were observed for *N*-(2-cyanoethyl)-substituted imidazolium halides (**16[Cl]** and **18[Cl]**, Fig. 4), and it has been suggested that the lone pair- and π-electrons of the nitrile functional group are capable of inter-ion interactions (as seen in the crystal structures of **10[Br]**, **4[NO$_3$]**, and **4[N(CN)$_2$]**) which may contribute to higher T_g values.[20] The cation–cation contacts observed in the crystal structures of the *N*-cyanoethyl-substituted **5[Br]** reinforces this claim, where such organization of the IL structure though hydrogen bonding can result in elevated T_g values. Finally, T_g values are generally lower for longer *N*-cyanoalkyl-functionalized salts (*e.g.*, *N*-(4-cyanobutyl), Fig. 4, top) in comparison with shorter analogs (*e.g.*, *N*-cyanomethyl, Fig. 4, bottom), similar to the *N*-alkyl chain-length effect previously described.[2]

As with the halide series, several *N*-methyl-substituted nitrate salts with shorter *N*-cyanoalkyl chains showed melting transitions (T_m = 103 °C, **4[NO$_3$]**; 62 °C **5[NO$_3$]**; 42 °C, **10[NO$_3$]**), again, presumably due to the more efficient packing of *N*-methyl- *vs.* *N*-butyl-substituted cations.[17] Also similar to the halide series, the glass transitions for nitrate salts were found to decrease with increasing *N*-cyanoalkyl chain length (considering nitrates, *N*-methyl: T_g = −47 °C, **5[NO$_3$]** *vs.* −56 °C, **6[NO$_3$]**; *N*-butyl: T_g = −43 °C, **11[NO$_3$]**; −52 °C, **12[NO$_3$]**; −59 °C, **13[NO$_3$]**). However, in contrast to halides, no significant differences were found for changes in chain length for longer *N*-cyanoalkyl-functionalized nitrate salts (compare T_g = −56 °C, **6[NO$_3$]**, −56 °C, **7[NO$_3$]**, and T_g = −59 °C,

13[NO_3], −59 °C, **14[NO_3]**), and only small differences were observed in glass transitions with variation between N-methyl- and N-butyl-substituted compounds.

One of the most visible trends in the DSC data resulted from a variation of the anion, where there was a high coincidence of low temperature T_g values for all *N*-(2-cyanoalkyl)-functionalized imidazolium dicyanamide salts (T_g = −67, **5[$N(CN)_2$]**; −62 °C, **17[$N(CN)_2$]**; −61 °C, **18[$N(CN)_2$]**; −66 °C, **19[$N(CN)_2$]**; −66 °C, **20[$N(CN)_2$]**). Interestingly, the *N*-methyl-substituted compounds **4-9[$N(CN)_2$]** showed much lower T_g when compared with analogous *N*-(2-cyanoethyl)-substituted products **16-20[$N(CN)_2$]**. It seems that the introduction of a second *N*-cyanoalkyl substituent in combination with the cyano groups present on the dicyanamide anion may have a synergistic effect for increasing T_g, possibly by increasing the interactions between ions through available π and lone-pair electrons from a total of four cyano groups per ion pair. In comparison to analogous halide and nitrate salts, however, ILs featuring the dicyanamide anion show the lowest T_g values reported here. This is in agreement with the literature, where dicyanamide-based ILs exhibit some of the lowest glass transition temperatures and broadest liquid ranges to date.[37]

Thermogravimetric analysis

In agreement with previous reports,[34,35] there was not a significant difference observed for the thermal stabilities of halides or nitrates when comparing *N*-methyl and *N*-butyl-substituted compounds within each series (**4–7**, **10-15[X]** and **4–7**, **10-15[NO_3]**, respectively). To illustrate this, the TGA traces for *N*-methyl and *N*-butyl-substituted salts are compared below in Fig. 5 and 6.

From analysis of the data in Fig. 5 and 6, the thermal stability for both *N*-methyl and *N*-butyl-substituted salts are also found to be similar for halide and nitrate analogs with longer *N*-cyanoalkyl chains; compare **6**, **7**, **13**, **14[NO_3]** and **[X]**, where all $T_{5\%onset}$ temperatures are *ca.* 250 °C as reported in Table 1. However, as the *N*-cyanoalkyl chain is shortened, there is a significant decrease in thermal stability observed for the nitrate salts (*e.g.*, compare $T_{5\%onset}$ = 183 °C, **4[NO_3]**; 166 °C, **5[NO_3]** (*N*-methyl) and $T_{5\%onset}$ = 168 °C, **11[NO_3]**; 180 °C, **12[NO_3]** (*N*-butyl)). Additionally, the *N*-(1-cyanoethyl)-substituted nitrate salts also showed reduced thermal stability (*e.g.*, $T_{5\%onset}$ = 168 °C, **10[NO_3]**; 157 °C, **15[NO_3]**) in comparison with *N*-cyanoalkyl-functionalized cations in the same series with longer chain lengths. Thus, *N*-cyanoalkyl-functionalized salts appear to be less stable in the nitrate form compared with analogous halides for shorter *N*-cyanoalkyl-functional groups. It is postulated that the proximity of the nitrile group to the formal charge of the imidazolium ring may have an activating effect for the decomposition pathway involving the nitrate anion that is not observed for halides. Increasing the proximity of the electron-withdrawing nitrile group to the imidazolium core may result in destabilization similar to that observed when nitrile groups are directly appended to the imidazolium core.[26]

N-(2-cyanoethyl)-substituted imidazolium halides **16-20[X]** were generally more stable than their *N*-methyl and *N*-butyl analogs (compare $T_{5\%onset}$ = 196 °C, **16[Cl]**; 206 °C, **4[Cl]**; 186 °C, **11[Cl]**). However, thermal stability is greatly reduced when comparing *N*-methyl to *N*-(2-cyanoethyl)-functionalized dicyanamide salts (>100 °C difference, see Fig. 7).

Considering the similarity of the $T_{5\%onset}$ values for the *N*-(2-cyanoethyl) salts **16-20[$N(CN)_2$]** (Fig. 7, right) with the 1-(2-cyanoethyl)-3-methylimidazolium dicyanamide salt, **5[$N(CN)_2$]** (Fig. 7, left), we can then consider the possibility that the 2-cyanoethyl substituent has a key role in the thermal degradation of the material. This same functional group is known as a facile leaving group in the deprotection step for the synthesis of 1-cyanoalkylimidazoles using heat under basic conditions,[39] and all *N*-(2-cyanoethyl)-*N*-cyanoalkyl-substituted dicyanamide salt thermal stabilities coincide with that found for *N*-(2-cyanoethyl)-functionalized **5[$N(CN)_2$]** ($T_{5\%onset}$ = 161 °C). Thus, without the *N*-(2-cyanoethyl) substituent (*e.g.*, *N*-methyl analogs), a more thermally-stable material results that shows initial mass loss at much higher temperatures. Halides featuring the *N*-(2-cyanoethyl) functionality showed low, uniform decomposition temperatures across the series. This observed uniformity is also found for the *N*-(2-cyanoethyl)-functionalized dicyanamide compounds, however, the $T_{5\%onset}$ values are much lower when compared with analogous halides ($T_{5\%onset}$ (range): 148–170 °C, see Table 1).

As can be noted from the comparative TGA plots provided here (Fig. 5–7), there are some ILs that did not completely decompose under the conditions of the TGA experiment.

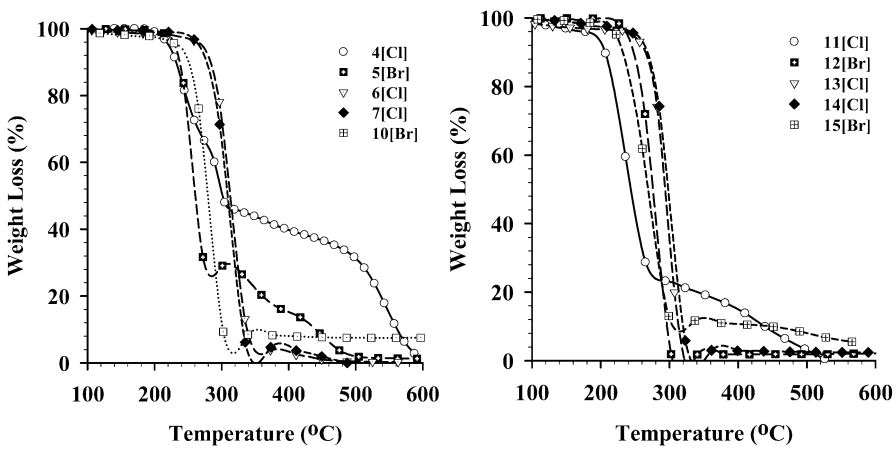

Fig. 5 Comparison of TGA data for *N*-methyl- (**4–7**, **10[X]**, left) and *N*-butyl-substituted (**11-15[X]**, right) halide salts.

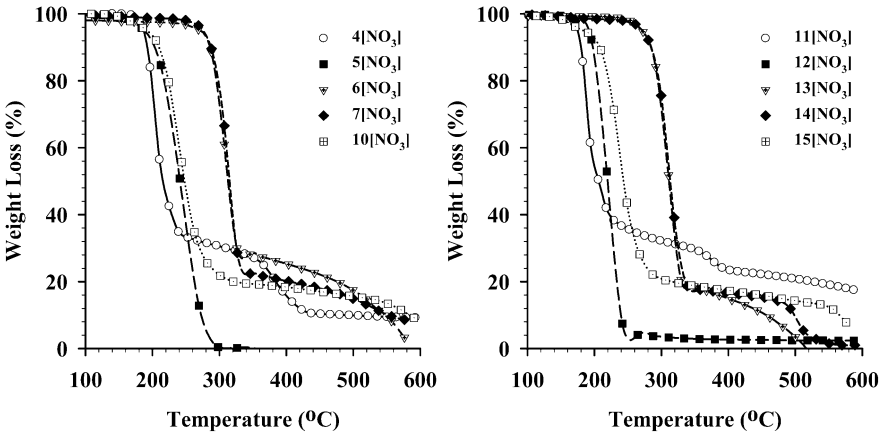

Fig. 6 Comparison of TGA data for *N*-methyl- (**4–7**, **10[NO$_3$]**, left) *vs.* *N*-butyl-substituted (**11-15[NO$_3$]**, right) nitrate salts.

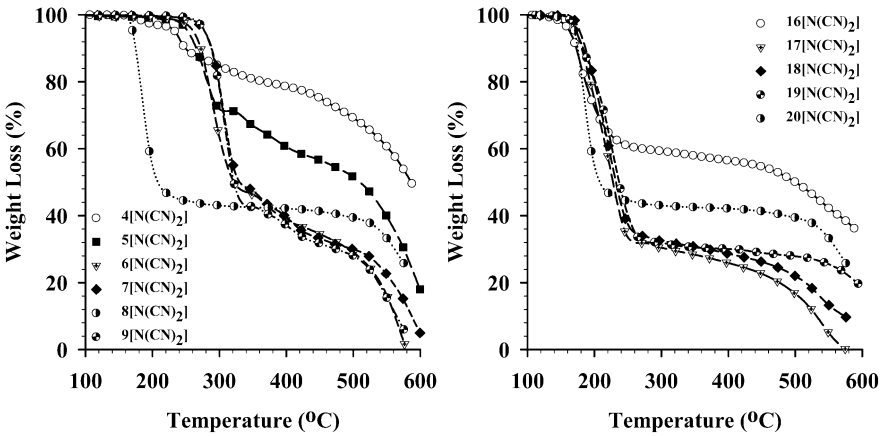

Fig. 7 Comparison of TGA plots for *N*-methyl- (**4-9[N(CN)$_2$]**, left) *vs.* *N*-(2-cyanoethyl)-substituted (**16-20[N(CN)$_2$]**, right) dicyanamide salts.

For the halide salts, those featuring short *N*-cyanoalkyl-functionalized cations (*e.g.*, **4**, **5**, **10**, **11**, **15[X]**) all showed a two-step decomposition pattern. Upon initial onset (as reported in Table 1), decomposition continued gradually from about 300 °C until reaching nearly 10–40% of original mass near 500 °C. For nitrate salts, all but the *N*-(2-cyanoethyl)-functionalized compounds (**5**, **12[NO$_3$]**) showed this trend, with around 10–30% of initial mass remaining. Char formation was especially pronounced for *N*-cyanomethyl (**4**, **11[NO$_3$]**) and *N*-(1-cyanoethyl)-functionalized (**10**, **15[NO$_3$]**) nitrate salts. Finally, the highest production of thermally stable material is evident for the dicyanamide salts, where all salts were found to result in char formation (30–80% mass). Upon visual inspection of the material in the TGA pan, the material appeared as a light-weight foam with a dark gray, metallic sheen.

There have been reports in the literature for similar formation of carbonaceous char from nitrile-functionalized imidazolium salts in the temperature ranges reported above, where cyclization of nitrile into carbonitride or nitrogen-doped graphene have found utility as microporous and mesoporous materials for catalyst support or chemical separation membranes.[74,75] The absence of char formation for **5[NO$_3$]** and **12[NO$_3$]** implies that, under the temperature and atmosphere of the TGA experiment, these nitrate salts preferentially undergo complete thermal decomposition rather than forming carbonaceous matter. Schnick[76,77] and MacFarlane[61] have indicated similar cyclization and polymerization of cyanamide and dicyanamide anions. The high productivity for char in all dicyanamide salts seems to be additive, where the nitrile groups from both *N*-cyanoalkyl, as well as the dicyanamide anion are available for reaction. As the weight percent of the carbonaceous material is variable depending on the type of cation, as well as the identity of the anion, there is potential application for these findings as a modular system for the design of porous materials for numerous applications.

Impact, friction, and electrostatic discharge sensitivity

All dicyanamide salts (**4–9**, **16-20[N(CN)$_2$]**) were found to be very insensitive (Table 1, last column). Drop-hammer testing results indicated a range of 170–200 kg cm and, when compared to impact sensitivity values of other known energetic materials such as TNT (98 kg cm), RDX (28 kg cm) and DNB (28 kg cm),[78] the salts reported here are considered to be insensitive to impact.

The results from both friction testing (no response at greater than 211 Newtons for the Julius Peters test) and electrostatic discharge testing (negative response at 1 Joule determined from use of Air Force Research Laboratory ESD apparatus) also provide evidence that these dicyanamide salt structures

exhibit low sensitivities. These properties would be appreciated in applications where non-sensitive liquids are desired (*e.g.*, fuels, lubricants).

Conclusions

The focus for this work was to explore the synthesis of new 1-alkyl-3-cyanoalkylimidazolium ILs and to examine the effects of different cation substituent lengths (*N*-alkyl, *N*-cyanoalkyl), as well as energetic anions (nitrate, dicyanamide) on the observed thermal properties for each salt reported. Most of the 41 compounds prepared were ILs by definition (melting point below 100 °C). DSC analyses indicated several distinct classes of thermal behavior, including liquid–liquid transitions from failed attempts for the salt to crystallize from a supercooled phase within the timeframe of the DSC experiment. This thermal behavior was most frequently observed for compounds with long *N*-alkyl and *N*-cyanoalkyl chain lengths, as well as for most dicyanamide salts.

Melting transitions were observed mainly for short-chain *N*-cyanoalkyl-functionalized cations, and the trends for T_g were generally the same with changing *N*-cyanoalkyl chain lengths. Nonetheless, the effects of *N*-alkyl chain length on T_g in general often depended on the type of anion present, where halides often showed a greater decrease in glass transition temperature than nitrates when comparing *N*-methyl *versus* *N*-butyl analogs. The dicyanamide salts had uniformly lower T_g values than analogous halides and nitrates, and the *N*-methyl-substituted dicyanamide ILs exhibited lower T_g values than *N*-(2-cyanoethyl)-functionalized salts.

There appeared to be considerably different trends in the observed $T_{5\%onset}$ values obtained by TGA with respect to changes in the *N*-alkyl substituent, the *N*-cyanoalkyl chain length, and the class of anion present. Halide salts with short *N*-cyanoalkyl substituents were less stable than the *N*-butyl analogs. Although the difference between *N*-methyl and *N*-butyl analogs of nitrate salts did not differ significantly, there was a much lower stability in short *N*-cyanoalkyl-functionalized nitrates in comparison with longer chain analogs.

For the dicyanamide-based ILs, all *N*-methyl substituted salts seemed to be very thermally stable in comparison with halides and nitrates. However, an exception to this was **5[N(CN)$_2$]** which showed a $T_{5\%onset}$ much lower than the others in the series. Recognizing the similarity in thermal decomposition behavior of **5[N(CN)$_2$]** with other *N*-(2-cyanoethyl)-functionalized compounds (**16-20[N(CN)$_2$]**), it is concluded that the cyanoethyl functionality may have a profound influence on the thermal decomposition pathway observed in the TGA experiment for these compounds. Furthermore, the prevalence of carbonaceous char for all compounds seemed to follow the anion trend $[X]^- < [NO_3]^- < [N(CN)_2]^-$, where all shorter *N*-cyanoalkyl-functionalized ILs for halides and nitrates exhibited a characteristic 2-step decomposition pattern. The exception to this was for *N*-(2-cyanoethyl)-functionalized nitrate salts (**5[NO$_3$]** and **12[NO$_3$]**), which showed complete decomposition without any residual material remaining.

Finally, in the case of the dicyanamide salts, the most char production was clearly evident, where up to 80% of the original weight was found to remain up to nearly 500 °C. As such, the *N*-cyanoalkyl-substituted imidazolium salts studied here suggest potential use as building blocks for porous mesoscale materials that can be further functionalized to provide a versatile scaffold for numerous applications (*e.g.*, heterogeneous catalysis, chemical separations, *etc.*).

Experimental

Materials and methods

Reagents were used as obtained from commercial sources (Sigma-Aldrich, Milwaukee, WI) unless otherwise noted. All solvents were 'solvent grade' and used as received without additional purification. BioRad AG 1-X8 (100–200 mesh with 8% divinylbenzene copolymer cross-linkage) strongly basic anion exchange resin was converted to $(NO_3)^-$-form from the commercially available $(Cl)^-$-form following the manufacturer's protocol,[45,46] where the resin was loaded into a glass chromatographic column (1 cm diameter × 10 cm tall), washed with 5 bed volumes of 0.5 N sodium nitrate solution, and the eluted solution was spot-checked for completeness of chloride removal with a 1.0 M silver nitrate solution. Final conditioning of the nitrate-exchanged resin column was completed by washing with 2 bed volumes of deionized water.

The ^{1}H and ^{13}C NMR spectra were recorded using Bruker AV-360 and AV-500 (Karlsruhe, Germany) spectrometers operating at 500 or 360 MHz and 90 or 125 MHz, respectively. Infrared (IR) analyses were obtained by direct measurement of the neat samples by utilizing a Perkin-Elmer 100 FT-IR instrument, Perkin-Elmer (Shelton, CT) featuring an attenuated total reflection (ATR) force gauge, and spectra were obtained in the range of ν_{max} = 650–4000 cm^{-1}.

Thermogravimetric Analyses (TGA) were performed using a TGA 2950, TA Instruments, Inc. (New Castle, DE). These experiments were conducted under air atmosphere and measured in the dynamic heating regime. Samples between 5–15 mg were heated from 30–600 °C under constant heating ramp of 5 °C min^{-1} with a 30 min isotherm at 75 °C. Temperatures reported for the decomposition profiles for all materials were established as the onset temperature for decomposition of the first 5% of the sample ($T_{5\%onset}$).

Melting point/glass transition analyses were performed by Differential Scanning Calorimetry (DSC) using a DSC 2920 Modulated DSC, TA Instruments, Inc. (New Castle, DE) cooled with a liquid nitrogen cryostat. The calorimeter was calibrated for temperature and cell constants using indium (T_m = 156.61 °C; C = 28.71 J g^{-1}). Data were collected at atmospheric pressure, where samples were initially heated at a rate of 5 °C min^{-1} to a temperature not to exceed 50 °C below the measured $T_{5\%onset}$ (obtained from TGA). The sample was then held for a 5 min isotherm prior to two cycles of cooling and heating (back to upper temperature limit from first heating) at a rate of 5 °C min^{-1} spaced by 5 min isothermal holding at lower (T = −100 °C, unless otherwise stated) and upper (as indicated above) endpoint temperatures. Samples between 5–15 mg were used in aluminum sample pans (sealed, then perforated with a pin-hole to equilibrate pressure resulting from potential expansion of evolved gases). The DSC was adjusted so that zero heat flow was between 0 and −0.5 mW,

and the baseline drift was less than 0.1 mW over the temperature range of 0–180 °C. An empty sample pan served as the reference. Temperatures reported for the glass transition (T_g) and melting (T_m) were established as the onset temperature for the endothermic change in heat flow measured through the material and as the onset temperature for the exothermic change in heat flow measured in the case of observed crystallization (T_{cryst}).

Impact sensitivity testing was performed at the Air Force Research Laboratory (Edwards Air Force Base, CA). Analysis was carried out on an Olin-Mathieson drop weight tester, where a small sample (20 mg) was placed in a standard sample cup (liquid or solid cell employed as appropriate), and a multi-kilogram mass was dropped vertically from measured heights upon the closed sample.[79–81] The drop height in centimetres was recorded, and the point was determined at which 50% of impacts were positive. A sample of water was used as a standard calibration for liquid samples, and 1,3,5-trinitroperhydro-1,3,5-triazine was used for calibration for solid samples.

For friction testing, a Julius-Peters friction tester was employed whereby a small amount of sample (20 mg) was placed on a small ceramic square plate and a steel pin was pushed across the sample under a known load. Any evidence of discoloration, odor, smoke, or spark was considered a positive test. All samples tested were insensitive to friction, showing negative response at greater than 211 Newton. Sensitivity to electrostatic discharge (ESD) was determined using the AFRL ESD test apparatus with initial sample test level at 5000 V with capacitance set to deliver 0.25 J. Each of the samples was determined to be insensitive to ESD, as they all showed negative response under 1 Joule when tested.

Single-crystal X-ray diffraction data were collected for compounds **5[Br]**, **10[Br]**, **4[NO_3]**, and **4[$N(CN)_2$]** on a Bruker SMART diffractometer equipped with a CCD area detector using graphite-monochromated Mo-Kα (λ = 0.71073 Å) radiation. Crystals were cooled to −100 °C during data collection. The structures were solved using the SHELXTL software package[82] and the absorption corrections were made with SADABS.[83] The structures were refined by full-matrix least-squares on F^2. Non-hydrogen atoms were located from the difference map and refined anisotropically. Hydrogen atoms were constrained to idealized positions except methyl hydrogen atoms which were refined using a riding rotating model.

Synthetic protocols

N-Cyanoalkyl-functionalized imidazolium halides (4-20[X])

General procedure to prepare **4[Cl]** *and* **11[Cl]**. Compounds **4[Cl]** and **11[Cl]** were each prepared based on a previous method.[42] Yields and reaction times were not optimized, and the following serves as a general procedure. In a 50 mL round bottom flask with a magnetic stirbar, chloroacetonitrile (10% molar excess) was slowly added to 1-alkylimidazole (**1** or **2**, respectively). The mixture was stirred at room temperature overnight, and the resulting product was washed with ethyl acetate (4 × 5 mL) and dried by rotary evaporation prior to final removal of residual solvent by high vacuum at room temperature for 24 h.

Caution. Chloroacetonitrile is a hazardous irritant/lachrymator potentially tumorigenic/teratogenic/mutagenic. Protective clothing/gloves and a properly ventilated workspace should be utilized when handling this material. Besides, this material is combustable as liquid or vapor, and scaled-up exothermic reactions with bases should be controlled by cooling. Please refer to Material Safety Data Sheet (MSDS) for further details (CAS # 107-14-2).

1-Cyanomethyl-3-methylimidazolium chloride (4[Cl]). Compound **4[Cl]** was prepared from **1** (2.870 g, 35 mmol). White solid, water soluble (90%); ^{1}H NMR (500 MHz, DMSO-d_6) δ ppm 9.56 (s, 1H), 8.00 (t, 1H), 7.87 (t, 1H), 5.82 (s, 2H), 3.92 (s, 3H); ^{13}C NMR (125 MHz, DMSO-d_6) δ ppm 138.3, 124.8, 123.0, 115.3, 37.2, 36.6. FT-IR (ν_{max} in cm^{-1}): 3392 (w), 3032 (s), 2977 (s), 2906 (s), 1575 (s), 1565 (s), 1439 (m), 1337 (m), 1254 (s), 1168 (s), 915 (m).

1-Butyl-3-cyanomethylimidazolium chloride (11[Cl]). Compound **11[Cl]** was prepared from **2** (2.612 g, 20 mmol). Amber liquid (57%); ^{1}H NMR (500 MHz, DMSO-d_6) δ ppm 9.70 (s, 1H), 8.04 (d, 1H), 7.99 (d, 1H), 5.83 (s, 2H), 4.27 (t, 2H), 1.75 (pent, 2H), 1.23 (hex, 2H), 0.88 (T, 3H); ^{13}C NMR (125 MHz, DMSO-d_6) δ ppm 137.2, 123.0, 122.6, 114.7, 48.8, 36.7, 31.1, 18.6, 13.1; FT-IR (ν_{max} in cm^{-1}): 3370 (b), 3135 (w), 3064 (m), 2960 (s) 2934 (s), 2874 (m), 1638 (w), 1558 (s), 1463 (m), 1420 (w), 1337 (w), 1251 (w), 1209 (w), 1163 (s), 1115 (w), 1030 (m), 926 (w), 872 (w), 755 (s), 708 (w), 662 (w).

General procedure to prepare 5-10, 12-15[X]. Compounds **5-10**, **12-15[X]** were obtained under solvent-free conditions as with **4[Cl]** and **11[Cl]**, but with the addition of heat during the reaction. Yields and reaction times were not optimized, and the following serves as a general procedure. To a 20 mL Ace Glass high temperature vial fitted with a Teflon screw-cap, the appropriate haloalkylnitrile (10% molar excess) was added to 1-alkylimidazole (**1** or **2**). Upon fastening the screw-cap on the vial, the mixture was stored in a furnace set to 70 °C for 48 h. As exceptions to this procedure, compound **5[Br]** was inadvertently left for 20 days in the furnace at 70 °C, and compound **12[Br]** was obtained from first preparing 1-(2-cyanoethyl)imidazole, **3**, by literature methods (see **3**, below),[39] which was then alkylated with 1-bromobutane in 10% molar excess. After each reaction was finished, the reaction mixtures were washed with ethyl acetate or acetone (4 × 5 mL) prior to drying first by rotary evaporation followed by removal of residual solvent by high vacuum for 24 h at room temperature.

1-(2-Cyanoethyl)imidazole (3). Compound **3** was prepared by combining imidazole (5.301 g, 100 mmol) with acrylonitrile (6.799 g, 110 mmol) in toluene (20 mL) and then adding triethylamine (1 mL). With the addition of a magnetic Teflon stir bar, the reaction mixture was stirred and heated to 50 °C and maintained at this temperature for 30 h when the product separated as a lower liquid phase from the toluene solution. Purification of **3** was achieved by removing the solvent from the lower product phase by first decanting and then washing the product phase of residual solvent and starting materials with 3 × 10 mL of acetone. After removal of residual solvent by rotary evaporation, final purification involved further

drying under high vacuum at room temperature for 24 h prior to use. Amber liquid (71%); ^{1}H NMR (500 MHz, DMSO-d_6) δ ppm 7.69 (s, 1H), 7.23 (t, 1H), 6.92 (t, 1H), 4.26 (t, 2H), 3.04 (t, 2H); ^{13}C NMR (125 MHz, DMSO-d_6) δ ppm 137.3, 128.7, 119.2, 118.5, 41.6, 19.5; FT-IR (ν_{max} in cm^{-1}): 3551 (m), 3473 (m), 3413 (w), 3240 (m), 3078 (w), 2966 (w), 2252 (w), 1616 (s), 1538 (m), 1410 (m), 1374 (m), 1376 (m), 1275 (m), 1231 (m), 1181 (m), 1116 (w), 1034 (w), 907 (m), 758 (m), 705 (m).

Caution. Acrylonitrile is a very hazardous irritant and permeator for skin and eyes, and requires protective clothing and a properly ventilated workspace. Prolonged exposure should be avoided, as there may be carcinogenic/teratogenic/mutagenic effects, as well as toxicity related to target organs including blood, liver, central nervous system, and kidneys. Additionally, explosive mixtures can be formed when vapors are allowed to mix with air, and accumulation of evaporated material is to be avoided. Please refer to Material Safety Data Sheet (MSDS) for further precautionary details (CAS #107-13-1).

1-(2-Cyanoethyl)-3-methylimidazolium bromide (5[Br]). Compound **5[Br]** was prepared from **1** (4.621 g, 38 mmol). Yellow solid (86%); ^{1}H NMR (500 MHz, DMSO-d_6) δ ppm 9.31 (s, 1H), 7.88 (s, 1H), 7.80 (s, 1H), 4.53 (t, 2H), 3.90 (s, 3H), 3.25 (t, 2H); ^{13}C NMR (125 MHz, DMSO-d_6) δ ppm 137.5, 124.4, 122.8, 118.2, 44.9, 36.5, 19.2; FT-IR (ν_{max} in cm^{-1}): 3139 (w), 3082 (s), 3042 (s), 2958 (w), 2845 (w), 2250 (w), 1780 (w), 1761 (w), 1727 (w), 1676 (w), 1575 (m), 1559 (w), 1448 (w), 1426 (w), 1401 (w), 1359 (w), 1341 (w), 1280 (w), 1199 (w), 1160 (s), 1092 (w), 1022 (w), 892 (w), 864 (s), 789 (s), 741 (s), 652 (m).

1-(3-Cyanopropyl)-3-methylimidazolium chloride (6[Cl]). Compound **6[Cl]** was prepared from **1** (3.610 g, 44 mmol). Yellow solid (92%); ^{1}H NMR (500 MHz, DMSO-d_6) δ ppm 9.42 (s, 1H), 7.87 (t, 1H), 7.78 (t, 1H), 4.28 (t, 2H), 3.86 (s, 3H), 2.61 (t, 2H), 2.14 (pent, 2H); ^{13}C NMR (125 MHz, DMSO-d_6) δ ppm 136.9, 123.5, 122.2, 119.5, 47.4, 35.6, 25.2, 13.4; FT-IR (ν_{max} in cm^{-1}): 3435 (s), 3371 (s), 3244 (w), 3126 (w), 3109 (w), 3063 (m), 2971 (w), 2938 (w), 2915 (w), 2839 (w), 2244 (m), 2186 (w), 2111 (w), 1731 (w), 1655 (w), 1619 (m), 1574 (s), 1562 (s), 1453 (m), 1425 (m), 1391 (w), 1344 (w), 1334 (w), 1325 (w), 1266 (w), 1160 (s), 1092 (s), 1017 (m), 867 (s), 850 (w), 774 (s), 723 (w), 665 (m).

1-(4-Cyanobutyl)-3-methylimidazolium chloride (7[Cl]). Compound **7[Cl]** was prepared from **1** (1.232 g, 15 mmol). Amber liquid (95%); ^{1}H NMR (500 MHz, DMSO-d_6) δ ppm = 9.24 (s, 1H), 7.82 (t, 1H), 7.75 (t, 1H), 4.24 (t, 2H), 3.86 (s, 3H), 2.57 (t, 2H), 1.87 (pent, 2H), 1.53 (pent, 2H); ^{13}C NMR (125 MHz, DMSO-d_6) δ ppm = 137.1, 124.1, 122.7, 120.9, 48.3, 36.3, 29.0, 22.0, 16.2; FT-IR (ν_{max} in cm^{-1}): 3372 (b), 3143 (w), 3058 (m), 2952 (w), 2869 (w), 2242 (w), 1637 (w), 1571 (s), 1458 (m), 1427 (w), 1385 (w), 1335 (w), 1293 (w), 1161 (s), 1091 (w), 1020 (w), 843 (w), 760 (m), 697 (w).

1-(5-Cyanopentyl)-3-methylimidazolium bromide (8[Br]). Compound **8[Br]** was prepared from **1** (1.724 g, 21 mmol). Amber liquid (94%); ^{1}H NMR (500 MHz, DMSO-d_6) δ ppm = 9.31 (s, 1H), 7.85 (s, 1H), 7.77 (s, 1H), 4.21 (t, 2H), 3.87 (s, 3H), 2.52 (t, 2H), 1.83 (pent, 2H), 1.59 (pent, 2H), 1.33 (pent, 2H); ^{13}C NMR (125 MHz, DMSO-d_6) δ ppm = 136.8, 123.8, 122.5, 120.8, 48.6, 36.0, 28.8, 24.7, 24.3, 16.3; FT-IR (ν_{max} in cm^{-1}): 3381 (b), 3141 (w), 3060 (m), 2936 (m), 2864 (w), 2242 (w), 1571 (s), 1459 (m), 1426 (m), 1362 (w), 1336 (w), 1167 (s), 1094 (w), 1029 (w), 835 (w), 755 (m), 697 (w).

1-(6-Cyanohexyl)-3-methylimidazolium bromide (9[Br]). Compound **9[Br]** was prepared from **1** (1.483 g, 18 mmol). Amber liquid (92%); ^{1}H NMR (500 MHz, DMSO-d_6) δ ppm = 9.23 (s, 1H), 7.82 (s, 1H), 7.74 (s, 1H), 4.18 (t, 2H), 3.87 (s, 3H), 2.50 (t, 2H), 1.80 (pent, 2H), 1.55 (pent, 2H), 1.37 (pent, 2H), 1.27 (pent, 2H); ^{13}C NMR (125 MHz, DMSO-d_6) δ ppm = 137.0, 124.1, 122.7, 121.1, 49.1, 36.2, 29.5, 27.8, 25.1, 24.9, 16.5; FT-IR (ν_{max} in cm^{-1}): 3417 (b), 3141 (w), 3059 (m), 2934 (m), 2861 (w), 2242 (w), 1731 (w), 1570 (s), 1459 (m), 1426 (m), 1365 (w), 1337 (w), 1297 (w), 1246 (w), 1164 (s), 1088 (w), 1046 (w), 1020 (w), 829 (m), 756 (m), 697 (w).

1-(1-Cyanoethyl)-3-methylimidazolium bromide (10[Br]). Compound **10[Br]** was prepared from **1** (0.615 g, 7.4 mmol). Yellow powder (85%); ^{1}H NMR (500 MHz, DMSO-d_6) δ ppm 9.53 (s, 1H), 8.12 (s, 1H), 7.79 (s, 1H), 6.17 (q, 1H), 3.90 (s, 3H), 1.90 (d, 3H); ^{13}C NMR (125 MHz, DMSO-d_6) δ ppm 137.5, 125.1, 121.4, 117.5, 45.7, 36.7, 19.5; FT-IR (ν_{max} in cm^{-1}): 3172 (w), 3150 (w), 3170 (w), 3043 (s), 3012 (s), 2882 (m), 2847 (w), 2618 (w), 2556 (w), 2249 (w), 1776 (w), 1735 (w), 1654 (w), 1580 (m), 1552 (s), 1448 (m), 1419 (m), 1381 (w), 1324 (w), 1302 (m), 1260 (w), 1182 (s), 1168 (s), 1100 (s), 1020 (m), 989 (w), 892 (w), 863 (s), 843 (m), 768 (s), 717 (m), 674 (w).

1-Butyl-3-(2-cyanoethyl)imidazolium bromide (12[Br]). Compound **12[Br]** was prepared by alkylation of **3** (1.521 g, 12 mmol) with 1-bromobutane (2.125 g, 15 mmol). Yellow solid (86%); ^{1}H NMR (500 MHz, DMSO-d_6) δ ppm 9.43 (s, 1H), 7.92 (d, 1H), 7.91 (d, 1H), 4.53 (t, 2H), 4.23 (t, 2H), 3.28 (t, 2H), 1.78 (pent, 2H), 1.24 (hex, 2H), 0.89 (t, 3H); ^{13}C NMR (125 MHz, DMSO-d_6) δ ppm 136.4, 122.6, 122.3, 117.5, 48.6, 44.3, 31.1, 18.5, 18.5, 13.1; FT-IR (ν_{max} in cm^{-1}): 3378 (b), 3134 (w), 3055 (m), 2960 (m), 2935 (m), 2875 (w), 1707 (m), 1640 (w), 1557 (s), 1463 (w), 1421 (w), 1362 (m), 1223 (w), 1160 (s), 1115 (w), 1020 (w), 925 (w), 871 (w), 754 (s), 708 (w).

1-(3-Cyanopropyl)-3-butylimidazolium chloride (13[Cl]). Compound **13[Cl]** was prepared from **2** (4.969 g, 40 mmol). Amber liquid (45%); ^{1}H NMR (500 MHz, DMSO-d_6) δ ppm 9.44 (s, 1H), 7.87 (s, 1H), 7.85 (s, 1H), 4.28 (t, 2H), 4.17 (t, 2H), 2.61 (t, 2H), 2.15 (pent, 2H), 1.78 (pent, 2H), 1.28 (sext, 2H), 0.90 (t, 3H); ^{13}C NMR (125 MHz, DMSO-d_6) δ ppm 136.3, 122.4, 122.3, 119.5, 48.5, 47.6, 31.1, 25.0, 18.7, 13.4, 13.2; FT-IR (ν_{max} in cm^{-1}): 3372 (b), 3134 (w), 3049 (m), 2959 (m), 2935 (m), 2873 (w), 2245 (s), 1639 (w), 1561 (s), 1370 (w), 1335 (w), 1163 (s), 1115 (w), 1054 (w), 1021 (w), 949 (w), 852 (m), 753 (m).

1-(4-Cyanobutyl)-3-butylimidazolium chloride (14[Cl]). Compound **14[Cl]** was prepared from **2** (1.870 g, 15 mmol). Amber liquid (97%); ^{1}H NMR (500 MHz, DMSO-d_6) δ ppm 9.62 (s, 1H), 7.91 (d, 1H), 7.90 (d, 1H), 4.27 (t, 2H), 4.20 (t, 2H), 2.59 (t, 2H), 1.89 (pent, 2H), 1.78 (pent, 2H), 1.53 (pent, 2H), 1.24 (sext, 2H), 0.89 (t, 3H); ^{13}C NMR (125 MHz, DMSO-d_6) δ ppm 136.2, 122.4, 122.3, 120.2, 48.7, 31.1, 28.3, 21.4, 18.6, 15.5, 13.1; FT-IR (ν_{max} in cm^{-1}): 3372 (b), 3131 (w), 3046 (m), 2957 (s), 2934 (s), 2872 (m), 2242 (w), 1638 (w), 1561 (s), 1458 (s), 1370

(w), 1333 (w), 1259 (w), 1160 (s), 1116 (w), 1050 (w), 1022 (w), 949 (w), 879 (m), 753 (s).

1-Butyl-3-(1-cyanoethyl)imidazolium bromide (15[Br]). Compound **15[Br]** was prepared from **2** (2.755 g, 22 mmol). Amber liquid (87%); ^{1}H NMR (500 MHz, DMSO-d_6) δ ppm 9.71 (s, 1H), 8.19 (s, 1H), 8.04 (s, 1H), 6.27 (q, 1H), 4.24 (t, 2H), 1.90 (d, 3H), 1.79 (pent, 2H), 1.27 (sext, 2H), 0.88 (t, 3H); ^{13}C NMR (125 MHz, DMSO-d_6) δ ppm 136.4, 123.3, 121.0, 117.0, 48.9, 46.2, 31.0, 18.7, 13.2; FT-IR (ν_{max} in cm^{-1}): 3126 (w), 3046 (s), 2959 (s), 2934 (s), 2873 (m), 2251 (w), 1691 (w), 1569 (m), 1551 (m), 1458 (m), 1381 (w), 1337 (w), 1315 (w), 1260 (w), 1210 (w), 1165 (s), 1115 (w), 1088 (w), 1021 (w), 983 (w), 948 (w), 842 (w), 752 (m).

1-(2-Cyanoethyl)-3-cyanomethylimidazolium chloride (16[Cl]). Compound **16[Cl]** was obtained from **3** (2.423 g, 20 mmol). White solid (87%); ^{1}H NMR (500 MHz, DMSO-d_6) δ ppm 7.82 (s, 1H), 4.51 (t, 2H), 3.14 (t, 2H), 2.74 (s, 2H); ^{13}C NMR (125 MHz, DMSO-d_6) δ ppm 146.0, 122.2, 118.3, 43.6, 18.6, 10.0; FT-IR (ν_{max} in cm^{-1}): 3327 (s), 3276 (s), 3167 (w), 3140 (w), 3126 (w), 3068 (m), 3036 (s), 2986 (m), 2954 (w), 2855 (w), 2254 (m), 1808 (w), 1693 (w), 1678 (w), 1651 (m), 1574 (w), 1561 (s), 1511 (w), 1449 (m), 1418 (m), 1404 (m), 1367 (w), 1349 (m), 1289 (m), 1238 (w), 1161 (s), 1113 (m), 1051 (w), 1020 (w), 1000 (w), 952 (w), 925 (m), 914 (m), 907 (m), 863 (s), 797 (s), 750 (m), 661 (s).

1-(3-Cyanopropyl)-3-(2-cyanoethyl)imidazolium chloride (17[Cl]). Compound **17[Cl]** was prepared from **3** (1.824 g, 15 mmol). Amber liquid (91%); ^{1}H NMR (500 MHz, DMSO-d_6) δ ppm 9.59 (s, 1H), 7.97 (s, 1H), 7.95 (s, 1H), 4.55 (t, 2H), 4.33 (t, 2H), 3.28 (t, 2H), 2.62 (t, 2H), 2.16 (pent, 2H); ^{13}C NMR (125 MHz, DMSO-d_6) δ ppm 137.5, 123.2, 123.1, 120.1, 118.2, 48.3, 44.9, 25.7, 19.1, 14.0; FT-IR (ν_{max} in cm^{-1}): 3370 (b), 3140 (w), 3058 (m), 2963 (w), 2906 (w), 2845 (w), 2248 (w), 1705 (w), 1638 (w), 1563 (s), 1450 (m), 1420 (m), 1358 (w), 1342 (w), 1229 (w), 1163 (s), 1109 (w), 1076 (w), 1050 (w), 1021 (w), 910 (w), 847 (w), 826 (w), 762 (s).

1-(4-Cyanobutyl)-3-(2-cyanoethyl)imidazolium chloride (18[Cl]). Compound **18[Cl]** was prepared from **3** (2.445 g, 20 mmol). Amber liquid (61%); ^{1}H NMR (500 MHz, DMSO-d_6) δ ppm 9.20 (s, 1H), 7.81 (s, 1H), 7.73 (s, 1H), 4.17 (t, 2H), 2.51 (t, 2H), 1.80 (pent, 2H), 1.55 (pent, 2H), 1.37 (pent, 2H), 1.27 (pent, 2H); ^{13}C NMR (125 MHz, DMSO-d_6) δ ppm 137.0, 124.1, 122.7, 121.1, 49.1, 36.2, 29.5, 27.8, 25.1, 16.5; FT-IR (ν_{max} in cm^{-1}): 3376 (b), 3137 (w), 3054 (m), 2958 (s), 2246 (w), 1639 (w), 1561 (s), 1455 (m), 1423 (m), 1363 (w), 1340 (w), 1236 (w), 1161 (s), 1052 (w), 1033 (w), 914 (w), 871 (w), 828 (w), 759 (s), 660 (w).

1-(5-Cyanopentyl)-3-(2-cyanoethyl)imidazolium bromide (19[Br]). Compound **19[Br]** was prepared from **3** (1.273 g, 10 mmol). Amber liquid (97%); ^{1}H NMR (500 MHz, DMSO-d_6) δ ppm 9.39 (s, 1H), 7.91 (d, 2H), 4.53 (t, 2H), 4.25 (t, 2H), 3.26 (t, 2H), 2.51 (t, 2H), 1.84 (pent, 2H), 1.59 (pent, 2H), 1.34 (pent, 2H); ^{13}C NMR (125 MHz, DMSO-d_6) δ ppm 137.0, 123.3, 123.0, 121.0, 118.2, 49.1, 45.0, 28.9, 24.5, 19.2, 16.5; FT-IR (ν_{max} in cm^{-1}): 3401 (s), 3140 (w), 3078 (m), 2940 (m), 2867 (w), 2246 (w), 1628 (m), 1561 (s), 1509 (w), 1458 (m), 1421 (m), 1363 (w), 1340 (w), 1290 (w), 1234 (w), 1158 (s), 1108 (w), 1083 (w), 1051 (w), 1033 (w), 915 (w), 826 (m), 754 (m), 660 (w).

1-(6-Cyanohexyl)-3-(2-cyanoethyl)imidazolium bromide (20[Br]). Compound **20[Br]** was prepared from **3** (1.067 g, 8.8 mmol). Amber liquid (86%); ^{1}H NMR (500 MHz, DMSO-d_6) δ ppm 9.36 (s, 1H), 7.89 (d, 2H), 4.52 (t, 2H), 4.23 (t, 2H), 3.25 (t, 2H), 2.51 (t, 2H), 1.81 (pent, 2H), 1.54 (pent, 2H), 1.35 (pent, 2H), 1.26 (pent, 2H); ^{13}C NMR (125 MHz, DMSO-d_6) δ ppm 137.0, 123.3, 123.0, 121.1, 118.2, 49.4, 44.9, 29.4, 27.8, 25.0, 24.9, 19.2, 16.5; FT-IR (ν_{max} in cm^{-1}): 3409 (b), 3135 (w), 3058 (m), 2838 (s), 2863 (m), 2244 (w), 1628 (w), 1561 (s), 1455 (s), 1422 (m), 1358 (w), 1340 (w), 1234 (w), 1161 (s), 1107 (w), 1052 (w), 1033 (w), 914 (w), 824 (w), 757 (s), 659 (w).

***N*-Cyanoalkyl-functionalized imidazolium nitrates (4–7, 9-15[NO$_3$])**

Preparation of nitrate-form of anion exchange resin. Strongly basic anion exchange resin (BioRad AG 1-X8, chloride form) was converted to nitrate form by successive washes of a loaded column ($\sim$8 cm^3 bed volume) with 1 N sodium nitrate solution. Each eluted fraction was tested with 0.1 M silver nitrate solution to visually indicate when the resin had been fully exchanged (*e.g.*, no silver chloride precipitate formed). Final conditioning of the nitrate resin column included washing with 2 bed volumes of deionized water.

General procedure for the exchange of halides for nitrate anion and product isolation, **4-7**, **9-15[NO$_3$]**. A solution of *N*-cyanoalkyl imidazolium halide salt (**4–7**, **9-15[X]**) was prepared based upon the calculated 'dry weight' capacity of the resin being used (2.6 meq/g dry resin). All halide salts were eluted as solutions in 100 mL of water though a prepared column of the nitrate-exchanger resin. All collected fractions were spot-tested with 0.1 M silver nitrate solution to confirm the absence of halide (*e.g.*, no precipitate shown) prior to combining and removing water, first by evaporation under air stream and then further drying under high vacuum overnight.

1-Cyanomethyl-3-methylimidazolium nitrate (4[NO$_3$]). Compound **4[NO$_3$]** was prepared from **4[Cl]** (1.063 g, 6.5 mmol). White solid (81%); ^{1}H NMR (500 MHz, DMSO-d_6) δ ppm 9.26 (s, 1H), 7.89 (t, 1H), 7.79 (t, 1H), 5.59 (s, 2H), 3.89 (s, 3H); ^{13}C NMR (125 MHz, DMSO-d_6) δ ppm 137.7, 124.3, 122.4, 114.6, 36.7, 36.0; FT-IR (ν_{max} in cm^{-1}): 3431 (b), 3154 (w), 3130 (w), 3088 (m), 3035 (m), 3011 (m), 2966 (w), 1789 (w), 1748 (w), 1662 (w) 1581 (m), 1561 (m), 1472 (w), 1457 (w), 1425 (m), 1413 (m), 1387 (m), 1328 (s), 1275 (s), 1166 (s), 11 087 (w), 1090 (w), 1041 (w), 1020 (w), 953 (w), 921 (w), 900 (s), 827 (m), 783 (m), 775 (m), 749 (m), 725 (w) 708 (w), 673 (w).

1-(2-Cyanoethyl)-3-methylimidazolium nitrate (5[NO$_3$]). Compound **5[NO$_3$]** was prepared from **5[Br]** (1.281 g, 5.9 mmol). Yellow solid (84%); ^{1}H NMR (500 MHz, DMSO-d_6) δ ppm 9.28 (s, 1H), 7.82 (t, 1H), 7.76 (t, 1H), 3.89 (s, 3H), 3.21 (t, 2H); ^{13}C NMR (125 MHz, DMSO-d_6) δ ppm 137.0, 123.9, 122.2, 117.6, 44.3, 35.8, 18.5; FT-IR (ν_{max} in cm^{-1}): 3156 (w), 3126 (w), 3088 (m), 3040 (m), 2258 (m), 1746 (w), 1664 (w), 1579 (m), 1566 (m), 1450 (w), 1426 (w), 1363 (m), 1332 (s), 1301 (m), 1176 (s), 1084 (w), 1042 (w), 1029 (w), 1016 (w), 943 (w), 888 (m), 877 (m), 827 (m), 775 (s), 748 (m), 706 (w), 657 (m).

1-(3-Cyanopropyl)-3-methylimidazolium nitrate (6[NO_3]). Compound **6[NO_3]** was prepared from **6[Cl]** (1.062 g, 5.7 mmol). Amber liquid (76%); ^{1}H NMR (500 MHz, DMSO-d_6) δ ppm 9.18 (s, 1H), 7.80 (t, 1H), 7.73 (t, 1H), 4.24 (t, 2H), 3.84 (s, 3H), 2.58 (t, 2H), 2.13 (pent, 2H); ^{13}C NMR (125 MHz, DMSO-d_6) δ ppm 136.8, 123.6, 122.2, 119.5, 47.5, 35.6, 25.1, 13.3; FT-IR (ν_{max} in cm^{-1}): 3151 (w), 3101 (m), 2960 (w), 2247 (w), 1745 (w), 1633 (w), 1576 (m), 1566 (m), 1451 (w), 1425 (w), 1327 (s), 1166 (s), 1084 (w), 1024 (w), 847 (w), 830 (m), 756 (m), 699 (w).

1-(4-Cyanobutyl)-3-methylimidazolium nitrate (7[NO_3]). Compound **7[NO_3]** was prepared from **7[Cl]** (0.644 g, 3.2 mmol). Amber liquid (83%); ^{1}H NMR (500 MHz, DMSO-d_6) δ ppm 9.17 (s, 1H), 7.78 (t, 1H), 7.72 (t, 1H), 4.21 (t, 2H), 3.85 (s, 3H), 2.54 (t, 2H), 1.87 (dt, 2H), 1.54 (dt, 2H); ^{13}C NMR (125 MHz, DMSO-d_6) δ ppm 136.6, 123.6, 122.1, 120.2, 47.8, 35.6, 28.4, 21.4, 15.5; FT-IR (ν_{max} in cm^{-1}): 3147 (w), 3100 (w), 2955 (w), 2244 (w), 1744 (w), 1574 (s), 1458 (w), 1426 (w), 1330 (s), 1216 (w), 1163 (w), 1084 (w), 1039 (w), 1024 (w), 854 (w), 830 (m), 754 (m), 698 (w).

1-(1-Cyanoethyl)-3-methylimidazolium nitrate (10[NO_3]). Compound **10[NO_3]** was prepared from **10[Br]** (1.314 g, 6.1 mmol). Yellow solid (95%); ^{1}H NMR (500 MHz, DMSO-d_6) δ ppm 9.44 (s, 1H), 8.09 (s, 1H), 7.85 (s, 1H), 6.05 (q, 1H), 3.89 (s, 3H), 1.89 (d, 3H); ^{13}C NMR (125 MHz, DMSO-d_6) δ ppm 137.0, 124.5, 120.8, 116.9, 45.1, 36.0, 18.8; FT-IR (ν_{max} in cm^{-1}): 3149 (w), 3097 (w), 2951 (w), 1747 (w), 1631 (w), 1581 (m), 1557 (m), 1452 (w), 1330 (s), 1261 (w), 1170 (s), 1090 (m), 1041 (w), 1021 (w), 984 (w), 842 (w), 829 (m) 755 (m), 718 (w).

1-Butyl-3-cyanomethylimidazolium nitrate (11[NO_3]). Compound **11[NO_3]** was prepared from **11[Cl]** (1.336 g, 6.5 mmol). Amber liquid (76%); ^{1}H NMR (500 MHz, DMSO-d_6) δ ppm 9.39 (s, 1H), 7.93 (t, 1H), 7.91 (t, 1H), 5.61 (s, 2H), 4.22 (t, 2H), 1.77 (pent, 2H), 1.26 (hext, 2H), 0.89 (t, 3H); ^{13}C NMR (125 MHz, DMSO-d_6) δ ppm 137.3, 123.1, 122.7, 114.6, 48.9, 36.8, 31.1, 18.7, 13.2; FT-IR (ν_{max} in cm^{-1}): 3142 (w), 3100 (w), 2963 (w), 2937 (w), 2875 (w), 2430 (w), 1789 (w), 1560 (w), 1325 (s), 1163 (s), 1115 (m), 1041 (w), 1033 (w), 1021 (w), 926 (w), 832 (s), 754 (m), 708 (w).

1-Butyl-3-(2-cyanoethyl)imidazolium nitrate (12[NO_3]). Compound **12[NO_3]** was prepared from **12[Br]** (1.544 g, 6.0 mmol). Amber liquid (94%); ^{1}H NMR (500 MHz, DMSO-d_6) δ ppm 9.34 (s, 1H), 7.88 (t, 1H), 7.86 (t, 1H), 4.51 (t, 2H), 4.22 (t, 2H), 3.23 (t, 2H), 1.77 (pent, 2H), 1.26 (sext, 2H), 0.88 (t, 3H); ^{13}C NMR (125 MHz, DMSO-d_6) δ ppm 136.5, 122.8, 122.4, 117.7, 48.7, 44.4, 31.2, 18.6, 18.5, 13.2; FT-IR (ν_{max} in cm^{-1}): 3140 (w), 3096 (w), 3038 (w), 2962 (w), 2935 (w), 2875 (w), 2252 (w), 1745 (w), 1631 (w), 1563 (m), 1459 (m), 1335 (s), 1163 (s), 1113 (w), 1041 (w), 1023 (w), 949 (w), 914 (w), 854 (w), 829 (w), 754 (w).

1-(3-Cyanopropyl)-3-butylimidazolium nitrate (13[NO_3]). Compound **13[NO_3]** was prepared from **13[Cl]** (1.305, 5.8 mmol). Amber liquid (83%); ^{1}H NMR (500 MHz, DMSO-d_6) δ ppm 9.28 (s, 1H), 7.83 (s, 1H), 7.82 (s, 1H), 4.26 (t, 2H), 4.17 (t, 2H), 2.59 (t, 2H), 2.15 (pent, 2H), 1.78 (pent, 2H), 1.26 (sext, 2H), 0.90 (t, 3H); ^{13}C NMR (125 MHz, DMSO-d_6) δ ppm 136.3, 122.5, 122.3, 119.5, 48.5, 47.7, 31.1, 25.0, 18.7, 13.3, 13.1; FT-IR (ν_{max} in cm^{-1}): 3140 (w), 3096 (w), 2961 (w), 2934 (w), 2875 (w), 2246 (w), 1744 (w), 1564 (m), 1459 (w), 1330 (s), 1162 (s), 1114 (w), 1084 (w), 1040 (w), 1026 (w), 949 (w), 852 (w), 830 (w), 753 (m), 708 (w).

1-(4-Cyanobutyl)-3-butylimidazolium nitrate (14[NO_3]). Compound **14[NO_3]** was prepared from **14[Cl]** (1.298 g, 5.4 mmol). Amber liquid (79%); ^{1}H NMR (500 MHz, DMSO-d_6) δ ppm 9.25 (s, 1H), 7.82 (d, 1H), 7.81 (d, 1H), 4.21 (t, 2H), 4.17 (t, 2H), 2.56 (t, 2H), 1.88 (dt, 2H), 1.79 (dt, 2H), 1.54 (dt, 2H), 1.26 (dt, 2H), 0.90 (t, 3H); ^{13}C NMR (125 MHz, DMSO-d_6) δ ppm 136.0, 122.4, 122.3, 120.2, 48.5, 47.9, 31.1, 28.3, 21.5, 18.7, 15.5, 13.1; FT-IR (ν_{max} in cm^{-1}): 3139 (w), 3093 (w), 2961 (w), 2934 (w), 2874 (w), 2244 (w), 1744 (w), 1564 (s), 1459 (m), 1330 (s), 1217 (w), 1160 (s), 1114 (w), 1084 (w), 1039 (w), 1026 (w), 949 (w), 857 (w), 830 (w), 753 (m), 707 (w).

1-Butyl-(1-cyanoethyl)imidazolium nitrate (15[NO_3]). Compound **15[NO_3]** prepared from **15[Br]** (1.673 g, 6.5 mmol). Amber liquid (89%); ^{1}H NMR (500 MHz, DMSO-d_6) δ ppm 9.49 (s, 1H), 8.12 (t, 1H), 7.95 (t, 1H), 6.01 (q, 1H), 4.21 (t, 2H), 1.90 (d, 3H), 1.79 (pent, 2H), 1.28 (sext, 2H), 0.90 (t, 3H); ^{13}C NMR (125 MHz, DMSO-d_6) δ ppm 136.4, 123.3, 121.0, 116.9, 49.0, 42.2, 31.0, 18.8, 18.7, 13.1; FT-IR (ν_{max} in cm^{-1}): 3253 (s), 3156 (m), 3118 (m), 3083 (m), 2878 (w), 1754 (w), 1587 (m), 1550 (m), 1470 (s), 1335 (m), 1309 (m), 1280 (m), 1162 (w), 1007 (s), 933 (m), 855 (w), 828 (w), 754 (w), 715 (w), 666 (w).

***N*-Cyanoalkyl-functionalized imidazolium dicyanamide salts (4–9, 16-20[$N(CN)_2$])**

General procedure to prepare **4–9**, **16-20[$N(CN)_2$]**. To a tared 100 mL round-bottom flask, halide precursor salts **4–9**, **16-20[X]** (2.8 to 18.7 mmol) were each dissolved in 40 mL deionized water. Silver dicyanamide was prepared by a literature method,[84] where sodium dicyanamide (15.290 g, 161 mmol) was added to an aqueous solution of silver nitrate (24.937 g, 147 mmol) at room temperature, and the mixture was stirred overnight in darkness. The solids were filtered and washed several times with water, and the washes were then combined with the filtrate prior to concentrating under air stream overnight and then further dried under high vacuum for 24 h. The prepared silver dicyanamide (1.1 equivalents) was added at room temperature to an aqueous solution of **4–9**, **16-20[$N(CN)_2$]** and homogenized using a magnetic Teflon stirbar prior to being brought to 50 °C in darkness and stirred for 1 h. The resulting yellowish/white solids were filtered and washed several times with water, and then the aqueous filtrate was concentrated under an air stream prior to final drying on high vacuum for 48 h at 60 °C. In addition to the routine characterization by NMR, FT-IR, TGA, and DSC, all dicyanamide samples were tested for impact and friction sensitivity.

1-Cyanomethyl-3-methylimidazolium dicyanamide (4[$N(CN)_2$]). Compound **4[$N(CN)_2$]** prepared from **4[Cl]** (2.510 g, 16 mmol). White solid (87%); ^{1}H NMR (500 MHz, DMSO-d_6) δ ppm = 9.24 (s, 1H), 7.88 (t, 1H), 7.78 (t, 1H), 5.58 (s, 2H), 3.98 (s, 3H); ^{13}C NMR (125 MHz, DMSO-d_6) δ ppm = 137.6, 124.2, 122.5, 119.0, 114.6, 36.7, 36.0; FT-IR (ν_{max} in cm^{-1}): 3681 (m), 3493

(w), 3149 (m), 3088 (m), 2953 (s), 2867 (w), 2230 (s), 2195 (m), 2125 (s), 1712 (w), 1612 (w), 1577 (w), 1558 (m) 1419 (w), 1410 (w), 1305 (s), 1218 (w), 1170 (s), 1111 (w), 1055 (m), 1033 (m), 933 (w), 906 (w), 857 (m), 745 (s); Impact sensitivity: >200 kg cm.

1-(2-Cyanoethyl)-3-methylimidazolium dicyanamide (5[N(CN)$_2$]). Compound **5[N(CN)$_2$]** prepared from **5[Br]** (3.591 g, 15 mmol). Amber liquid (74%); ^{1}H NMR (500 MHz, DMSO-d_6) δ ppm = 9.11 (s, 1H), 7.80 (t, 1H), 7.48 (t, 1H), 4.50 (t, 2H), 3.89 (s, 3H) 3.19 (s, 2H); ^{13}C NMR (125 MHz, DMSO-d_6) δ ppm = 136.9, 123.9, 122.2, 119.0, 117.6, 43.3, 35.8, 18.5; FT-IR (ν_{max} in cm^{-1}): 3681 (m), 3494 (w), 3150 (w), 3108 (m), 2967 (m), 2865 (w), 2229 (s), 2192 (m), 2119 (s), 1577 (m), 1562 (m) 1455 (w), 1420 (w), 1306 (s), 1165 (s), 1108 (w), 1053 (m), 1033 (m), 904 (w), 844 (m), 750 (m); Impact sensitivity: 172 kg cm.

1-(3-Cyanopropyl)-3-methylimidazolium dicyanamide (6[N(CN)$_2$]). Compound **6[N(CN)$_2$]** prepared from **6[Cl]** (1.560 g, 7.2 mmol). Amber liquid (93%); ^{1}H NMR (500 MHz, DMSO-d_6) δ ppm = 9.11 (s, 1H), 7.76 (s, 1H), 7.70 (s, 1H), 4.23 (t, 2H), 3.84 (s, 3H), 2.57 (t, 2H), 2.13 (m, 2H); ^{13}C NMR (125 MHz, DMSO-d_6) δ ppm = 136.7, 123.6, 122.2, 119.5, 47.6, 35.7, 25.1, 13.4; FT-IR (ν_{max} in cm^{-1}): 3681 (m), 3428 (m), 3152 (w), 3108 (w), 3010 (w), 2966 (m), 2866 (w), 2233 (s), 2196 (m), 2125 (s), 1632 (w), 1575 (m), 1565 (m) 1454 (w), 1425 (w), 1309 (s), 1166 (s), 1054 (m), 1033 (m), 1015 (w), 905 (w), 843 (w), 751 (m); Impact sensitivity: 170 kg cm.

1-(4-Cyanobutyl)-3-methylimidazolium dicyanamide (7[N(CN)$_2$]). Compound **7[N(CN)$_2$]** prepared from **7[Cl]** (0.563 g, 2.8 mmol). Amber liquid (83%); ^{1}H NMR (500 MHz, DMSO-d_6) δ ppm = 9.10 (s, 1H), 7.76 (t, 1H), 7.71 (t, 1H), 4.20 (t, 2H), 3.85 (s, 3H), 2.55 (q, 2H), 1.87 (m, 2H), 1.55 (m, 2H); ^{13}C NMR (125 MHz, DMSO-d_6) δ ppm = 136.5, 123.6, 122.1, 120.2, 119.0, 47.8, 35.7, 28.4, 21.4, 15.6; FT-IR (ν_{max} in cm^{-1}): 3681 (m), 3489 (w), 3149 (w), 3104 (w), 3011 (w), 2950 (m), 2867 (w), 2227 (s), 2192 (m), 2125 (s), 1623 (w), 1574 (m), 1456 (w), 1425 (w), 1305 (s), 1163 (s), 1055 (m), 1033 (w), 1017 (w), 903 (w), 842 (w), 749 (m); Impact sensitivity: 170 kg cm.

1-(5-Cyanopentyl)-3-methylimidazolium dicyanamide (8[N(CN)$_2$]). Compound **8[N(CN)$_2$]** prepared from **8[Br]** (2.299 g, 8.9 mmol). Amber liquid (84%); ^{1}H NMR (500 MHz, DMSO-d_6) δ ppm = 9.11 (s, 1H), 7.77 (t, 1H), 7.71 (t, 1H), 4.18 (t, 2H), 3.86 (s, 3H), 2.51 (t, 2H), 1.82 (m, 2H), 1.60 (m, 2H), 1.34 (m, 2H); ^{13}C NMR (125 MHz, DMSO-d_6) δ ppm = 136.4, 123.5, 122.1, 120.4, 119.0, 48.3, 35.6, 28.4, 24.4, 23.9, 15.8; FT-IR (ν_{max} in cm^{-1}): 3681 (w), 3491 (w), 3149 (w), 3104 (w), 3011 (w), 2941 (m), 2866 (w), 2227 (s), 2192 (m), 2125 (s), 1624 (w), 1574 (m), 1460 (w), 1425 (w), 1304 (s), 1168 (s), 1055 (m), 1033 (w), 1017 (w), 903 (w), 841 (w), 751 (m); Impact sensitivity: 170 kg cm.

1-(6-Cyanohexyl)-3-methylimidazolium dicyanamide (9[N(CN)$_2$]). Compound **9[N(CN)$_2$]** was prepared from **9[Br]** (1.973 g, 7.2 mmol). Amber liquid (87%); ^{1}H NMR (500 MHz, DMSO-d_6) δ ppm = 9.10 (s, 1H), 7.76 (s, 1H), 7.69 (s, 1H), 4.16 (t, 2H), 3.85 (s, 3H), 2.48 (t, 2H), 1.80 (m, 2H), 1.56 (m, 2H), 1.40 (m, 2H), 1.34 (m, 2H); ^{13}C NMR (125 MHz, DMSO-d_6) δ ppm = 136.4, 123.5, 122.1, 120.5, 190.0, 48.6, 35.6, 29.0, 27.3, 24.6, 24.4, 15.9; FT-IR (ν_{max} in cm^{-1}): 3667 (w), 3490 (w), 3149 (w), 3104 (w), 2938 (m), 2865 (w), 2230 (s), 2194 (m), 2125 (s), 1625 (w), 1573 (m), 1460 (w), 1425 (w), 1308 (s), 1167 (s), 1055 (m), 1033 (w), 903 (w), 842 (w), 753 (m); Impact sensitivity: 170 kg cm.

1-(2-Cyanoethyl)-3-cyanomethylimidazolium dicyanamide (16[N(CN)$_2$]). Compound **16[N(CN)$_2$]** was prepared from **16[Cl]** (1.487 g, 7.5 mmol). Amber liquid (88%); ^{1}H NMR (500 MHz, DMSO-d_6) δ ppm = 9.38 (s, 1H), 7.96 (t, 1H), 7.91 (t, 1H), 5.63 (s, 2H), 4.56 (t, 2H), 3.21 (s, 2H); ^{13}C NMR (125 MHz, DMSO-d_6) δ ppm = 138.3, 123.7, 123.6, 119.6, 118.1, 115.1, 45.3, 37.6, 19.0; FT-IR (ν_{max} in cm^{-1}): 3427 (w), 3145 (w), 3114 (w), 3015 (w), 2981 (w), 2233 (s), 2195 (m), 2125 (s), 1692 (w), 1623 (w), 1562 (m), 1457 (w), 1418 (w), 1310 (s), 1233 (w), 1164 (s), 1107 (w), 1080 (w), 1027 (w), 909 (w), 846 (w), 747 (m); Impact sensitivity: 176 kg cm.

1-(3-Cyanopropyl)-3-(2-cyanoethyl)imidazolium dicyanamide (17[N(CN)$_2$]). Compound **17[N(CN)$_2$]** was prepared from **17[Cl]** (4.823 g, 18 mmol). Amber liquid (92%); ^{1}H NMR (500 MHz, DMSO-d_6) δ ppm = 9.26 (s, 1H), 7.85 (t, 1H), 7.84 (t, 1H), 4.50 (t, 2H), 4.29 (t, 2H), 3.19 (t, 2H), 2.58 (t, 2H), 2.15 (m, 2H); ^{13}C NMR (125 MHz, DMSO-d_6) δ ppm = 136.7, 122.7, 122.5, 119.4, 119.0, 117.6, 47.8, 44.4, 25.1, 18.5, 13.4; FT-IR (ν_{max} in cm^{-1}): 3491 (w), 3144 (w), 3108 (w), 3015 (w), 2967 (w), 2229 (s), 2193 (m), 2125 (s), 1624 (w), 1564 (m), 1504 (w), 1452 (w), 1420 (w), 1306 (s), 1233 (w), 1161 (s), 1108 (w), 1079 (w), 1047 (w), 1023 (w), 906 (w), 844 (w), 750 (m); Impact sensitivity: 176 kg cm.

1-(4-Cyanobutyl)-3-(2-cyanoethyl)imidazolium dicyanamide (18[N(CN)$_2$]). Compound **18[N(CN)$_2$]** was prepared from **18[Cl]** (1.541 g, 6.0 mmol). Amber liquid (91%); ^{1}H NMR (500 MHz, DMSO-d_6) δ ppm = 9.25 (s, 1H), 7.84 (s, 2H), 4.50 (t, 2H), 4.26 (t, 2H), 3.20 (t, 2H), 2.55 (t, 2H), 1.89 (m, 2H), 1.55 (m, 2H); ^{13}C NMR (125 MHz, DMSO-d_6) δ ppm = 136.5, 122.7, 122.5, 120.2. 119.0, 117.6, 48.1, 44.4, 28.4, 21.4, 18.5, 15.6; FT-IR (ν_{max} in cm^{-1}): 3697 (w), 3665 (w), 3488 (w), 3144 (w), 2981 (m), 2939 (m), 2923 (m), 2866 (m), 2844 (m), 2233 (s), 2195 (m), 2125 (s), 1631 (w), 1563 (m), 1509 (w), 1455 (w), 1420 (w), 1310 (s), 1239 (w), 1159 (s), 1107 (w), 1055 (s), 1033 (s), 1016 (s), 908 (w), 827 (w), 748 (m); Impact sensitivity: 174 kg cm.

1-(5-Cyanopentyl)-3-(2-cyanoethyl)imidazolium dicyanamide (19[N(CN)$_2$]). Compound **19[N(CN)$_2$]** was prepared from **19[Br]** (2.247 g, 7.6 mmol). Amber liquid (85%); ^{1}H NMR (500 MHz, DMSO-d_6) δ ppm = 9.26 (s, 1H), 7.85(s, 2H), 4.50 (t, 2H), 4.24 (t, 2H), 3.21 (t, 2H), 2.49 (t, 2H), 1.84 (m, 2H), 1.60 (m, 2H), 1.36 (m, 2H); ^{13}C NMR (125 MHz, DMSO-d_6) δ ppm = 136.4, 122.7, 122.4, 120.4, 119.0, 117.6, 48.5, 28.4, 24.4, 23.9, 18.6, 15.9; FT-IR (ν_{max} in cm^{-1}): 3707 (w), 3681 (w), 3488 (w), 3144 (w), 2981 (m), 2967 (m), 2939 (m), 2866 (m), 2844 (m), 2229 (s), 2193 (m), 2125 (s), 1563 (m), 1509 (w), 1455 (w), 1420 (w), 1345 (m), 1308 (s), 1160 (s), 1055 (s), 1033 (s), 1016 (s), 906 (w), 826 (w), 749 (m); Impact sensitivity: 174 kg cm.

1-(6-Cyanohexyl)-3-(2-cyanoethyl)imidazolium dicyanamide (20[N(CN)$_2$]). Compound **20[N(CN)$_2$]** was prepared from **20[Br]** (1.401 g, 4.5 mmol). Amber liquid (85%); ^{1}H NMR

(500 MHz, DMSO-d_6) δ ppm = 9.25 (s, 1H), 7.85(q, 2H), 4.49 (t, 2H), 4.21 (t, 2H), 3.21 (t, 2H), 2.49 (t, 2H), 1.80 (m, 2H), 1.54 (m, 2H), 1.36 (m, 2H), 1.22 (m, 2H); ^{13}C NMR (125 MHz, DMSO-d_6) δ ppm = 136.4, 122.7, 122.4, 120.5, 119.0, 117.6, 48.8, 44.4, 28.9, 27.2, 24.5, 24.3, 18.6, 15.9; FT-IR (ν_{max} in cm^{-1}): 3697 (w), 3681 (w), 3489 (w), 3144 (w), 2966 (m), 2939 (m), 2866 (m), 2844 (m), 2231 (s), 2194 (m), 2125 (s), 1624 (w), 1563 (m), 1508 (w), 1455 (w), 1421 (w), 1308 (s), 1162 (s), 1055 (s), 1033 (s), 1017 (s), 906 (w), 825 (w), 752 (m); Impact sensitivity: 170 kg cm.

Acknowledgements

This research was supported by the Air Force Office of Scientific Research (Grant FA9550-10-1-0521).

References

1 T. M. Klapötke and G. Holl, *Green Chem.*, 2001, **3**, G75.
2 P. Wasserscheid and W. Keim, *Angew. Chem., Int. Ed.*, 2000, **39**, 3772.
3 J. M. Tishkoff and M. R. Berman, *40th AIAA Aerospace Sciences Meeting & Exhibit*, Reno, NV, 2002.
4 G. W. Drake, T. Hawkins, A. Brand, L. Hall, M. Mckay, A. Vij and I. Ismail, *Propellants, Explos., Pyrotech.*, 2003, **28**, 174.
5 R. P. Singh, R. D. Verma, D. T. Meshri and J. M. Shreeve, *Angew. Chem., Int. Ed.*, 2006, **45**, 3584.
6 M. Smiglak, A. Metlen and R. D. Rogers, *Acc. Chem. Res.*, 2007, **40**, 1182.
7 G. Steinhauser and T. M. Klapötke, *Angew. Chem., Int. Ed.*, 2008, **47**, 3330.
8 S. Trohalaki, R. Pachter, G. W. Drake and T. Hawkins, *Energy Fuels*, 2005, **19**, 279.
9 H. Xue and J. M. Shreeve, *Adv. Mater.*, 2005, **17**, 2142.
10 D. D. Zorn, J. A. Boatz and M. S. Gordon, *J. Phys. Chem. B*, 2006, **110**, 11110.
11 C. Ye and J. M. Shreeve, *J. Phys. Chem. A*, 2007, **111**, 1456.
12 J. C. Galvez-Ruiz, G. Holl, K. Karaghiosoff, T. M. Klapötke, K. Loehnwitz, P. Mayer, H. Noeth, K. Polborn, C. J. Rohbogner, M. Suter and J. J. Weigand, *Inorg. Chem.*, 2005, **44**, 4237.
13 H. Xue, Y. Gao, B. Twamley and J. M. Shreeve, *Inorg. Chem.*, 2005, **44**, 5068.
14 M. W. Schmidt, M. S. Gordon and J. A. Boatz, *J. Phys. Chem. A*, 2005, **109**, 7285.
15 P. F. Pagoria, G. S. Lee, A. R. Mitchell and R. D. Schmidt, *Thermochim. Acta*, 2002, **384**, 187.
16 H. Gao, C. Ye, O. D. Gupta, J.-C. Xiao, M. A. Hiskey, B. Twamley and J. M. Shreeve, *Chem.–Eur. J.*, 2007, **13**, 3853.
17 T. M. Klapötke and J. Stierstorfer, *Dalton Trans.*, 2009, 643.
18 S. Date, N. Itadzu, T. Sugiyama, Y. Miyata, K. Iwakuma, M. Abe, K. Yoshitake, S. Nishi and K. Hasue, *Sci. Technol. Ener. Mater.*, 2009, **70**, 152.
19 S. Schneider, T. Hawkins, M. Rosander, G. Vaghjiani, S. Chambreau and G. Drake, *Energy Fuels*, 2008, **22**, 2871.
20 S. D. Chambreau, S. Schneider, M. Rosander, T. Hawkins, C. J. Gallegos, M. F. Pastewait and G. L. Vaghjiani, *J. Phys. Chem. A*, 2008, **112**, 7816.
21 H. Gao, Y.-H. Joo, B. Twamley, Z. Zhou and J. M. Shreeve, *Angew. Chem., Int. Ed.*, 2009, **48**, 2792.
22 Y.-H. Joo, H. Gao, Y. Zhang and J. M. Shreeve, *Inorg. Chem.*, 2010, **49**, 3282.
23 Y. Zhang, H. Gao, Y. Guo, Y.-H. Joo and J. M. Shreeve, *Chem.–Eur. J.*, 2010, **16**, 3114.
24 A. R. Katritzky, S. Singh, K. Kirichenko, J. D. Holbrey, M. Smiglak, W. M. Reichert and R. D. Rogers, *Chem. Commun.*, 2005, 868.
25 A. R. Katritzky, S. Singh, K. Kirichenko, M. Smiglak, J. D. Holbrey, W. M. Reichert, S. K. Spear and R. D. Rogers, *Chem.–Eur. J.*, 2006, **12**, 4630.
26 A. R. Katritzky, H. Yang, D. Zhang, K. Kirichenko, M. Smiglak, J. D. Holbrey, W. M. Reichert and R. D. Rogers, *New J. Chem.*, 2006, **30**(3), 349.
27 M. Smiglak, N. J. Bridges, M. Dilip and R. D. Rogers, *Chem.–Eur. J.*, 2008, **36**, 11314.
28 M. Smiglak, C. C. Hines, T. B. Wilson, S. Singh, A. S. Vincek, K. Kirichenko, A. R. Katritzky and R. D. Rogers, *Chem.–Eur. J.*, 2010, **16**, 1572.
29 Y. Gao, H. Gao, C. Piekarski and J. M. Shreeve, *Eur. J. Inorg. Chem.*, 2007, 4965.
30 D. B. Zhao, Z. F. Fei, R. Scopelliti and P. J. Dyson, *Inorg. Chem.*, 2004, **43**, 2197.
31 Q. Zhang, Z. Li, J. Zhang, S. Zhang, L. Zhu, J. Yang, X. Zhang and Y. Deng, *J. Phys. Chem. B*, 2007, **111**, 2864.
32 S.-K. Fu and S.-T. Liu, *Synth. Commun.*, 2006, **36**, 2059.
33 F. Mazille, Z. Fei, D. Kuang, D. Zhao, S. M. Zakeeruddin, M. Grätzel and P. J. Dyson, *Inorg. Chem.*, 2006, **45**, 1585.
34 J. G. Huddleston, A. E. Visser, W. M. Reichert, H. D. Willauer, G. A. Broker and R. D. Rogers, *Green Chem.*, 2001, **3**, 156.
35 J. D. Holbrey and K. R. Seddon, *J. Chem. Soc., Dalton Trans.*, 1999, 2133.
36 C. Oommen and S. R. Jain, *J. Hazard. Mater.*, 1999, **67**, 253.
37 D. R. MacFarlane, J. Golding, S. Forsyth, M. Forsyth and G. B. Deacon, *Chem. Commun.*, 2001, 1430.
38 D. M. Drab, J. L. Shamshina, M. Smiglak, C. C. Hines, D. B. Cordes and R. D. Rogers, *Chem. Commun.*, 2010, **46**, 3544.
39 A. Horvath, *Synthesis*, 1994, **1**, 102.
40 H. Olivier-Bourbigou and F. Favre, in *Ionic Liquids in Synthesis*, ed. P. Wasserscheid and T. Welton, Wiley-VCH, New York, 2008, 2nd edn, pp. 490–491.
41 P. B. Hitchcock, K. R. Seddon and T. Welton, *J. Chem. Soc., Dalton Trans.*, 1993, 2639.
42 W. A. Herrmann, L. J. Goossen and M. Spiegler, *Organometallics*, 1998, **17**, 2162.
43 G. Tao, M. Zou, X. Wang, Z. Chen, D. G. Evans and Y. Kou, *Aust. J. Chem.*, 2005, **58**, 327.
44 S.-M. Gong, H.-Y. Ma, X.-H. Wan, Y.-F. Zhao, J.-Y. He and Q.-F. Zhou, *Gaodeng Xuexiao Huaxue Xuebao*, 2006, **27**, 761.
45 AG 1, AG MP-1 and AG 2 Strong Anion Exchange Resin:Instruction Manual, BioRad Laboratories: Hercules, CA (LIT212 Rev C; accessed online August 17, 2010; http://www.biorad.com/webroot/web/pdf/lsr/literature/9114_AG_1.pdf).
46 I. Dinares, C. Garcia de Miguel, A. Ibanez, N. Mesquida and E. Alcalde, *Green Chem.*, 2009, **11**, 1507.
47 N. Gathergood, M. T. Garcia and P. J. Scammells, *Green Chem.*, 2004, **6**, 166.
48 B. Clare, A. Sirwardana and D. R. MacFarlane, *Top. Curr. Chem.*, 2009, **290**, 1.
49 G. W. Drake, K. Tollison, L. Hall and T. Hawkins, in *Ionic Liquids III: Fundamentals, Progress, Challenges and Opportunities*, ed. R. Rogers and K. Seddon, American Chemical Society, Washington, DC, 2005.
50 B. V. Lotsch and W. Schnick, *Chem. Mater.*, 2005, **17**, 3976.
51 G. Svehla, *Vogel's Qualitative Inorganic Analysis*, Longman Scientific & Technical, Essex, UK, 1987, 6th edn, pp. 174–178.
52 A. R. Toral, A. P. de los Ríos, F. J. Hernández, M. H. A. Janssen, R. Schoevaart, F. van Rantwijk and R. A. Sheldon, *Enzyme Microb. Technol.*, 2007, **40**, 1095.
53 H. Zhao, G. A. Baker, Z. Song, O. Olubajo, L. Zanders and S. M. Campbell, *J. Mol. Catal. B: Enzym.*, 2009, **57**, 149.
54 S. Tang and A. V. Mudring, *Eur. J. Inorg. Chem.*, 2009, 1145.
55 A. J. Seeber, M. Forsyth, C. M. Forsyth, S. A. Forsyth, G. Annat and D. R. MacFarlane, *Phys. Chem. Chem. Phys.*, 2003, **5**, 2692.
56 T. Endo and K. Nishikawa, *J. Phys. Chem. A*, 2008, **112**, 7543.
57 W. L. Hough, M. Smiglak, H. Rodriguez, R. P. Swatloski, S. K. Spear, D. T. Daly, J. Pernak, J. E. Grisel, R. D. Carliss, M. D. Soutullo, J. J. H. Davis and R. D. Rogers, *New J. Chem.*, 2007, **31**(8), 1429.
58 R. Kurita and H. Tanaka, *Science*, 2004, **306**, 845.
59 K. Murata and H. Tanaka, *Nature Commun.*, 2010, **1**, 16.
60 C. P. Fredlake, J. M. Crosthwaite, D. G. Hert, S. N. V. K. Aki and J. F. Brennecke, *J. Chem. Eng. Data*, 2004, **49**, 954.
61 T. J. Wooster, K. M. Johanson, K. J. Fraser, D. R. MacFarlane and J. L. Scott, *Green Chem.*, 2006, **8**, 691.

62 I. Krossing, J. M. Slattery, C. Daguenet, P. J. Dyson, A. Oleinikova and H. Weingartner, *J. Am. Chem. Soc.*, 2006, **128**, 13427.
63 M. Smiglak, *PhD Dissertation*, The University of Alabama, 2007.
64 S. Jayaraman and E. J. Maginn, *J. Chem. Phys.*, 2007, **127**, 214504.
65 K. Nishikawa, S. Wang, H. Katayanagi, S. Hayashi, H. Hamaguchi, Y. Koga and K. Tozaki, *J. Phys. Chem. B*, 2007, **111**, 4894.
66 D. R. MacFarlane, J. Huang and M. Forsyth, *Nature*, 1999, **402**, 792.
67 D. R. MacFarlane and M. Forsyth, *Adv. Mater.*, 2001, **13**, 957.
68 J. M. Pringle, P. C. Howlett, D. R. MacFarlane and M. Forsyth, *J. Mater. Chem.*, 2010, **20**, 2056.
69 J. M. Pringle, J. Adebahr, D. R. MacFarlane and M. Forsyth, *Phys. Chem. Chem. Phys.*, 2010, **12**, 7234.
70 R. Lungwitz and S. Spange, *New J. Chem.*, 2008, **32**, 392.
71 E. I. Izgorodia, M. Forsyth and D. R. MacFarlane, *Aust. J. Chem.*, 2007, **60**, 15.
72 D. Kun, Z. Suojiang, W. Daxi and Y. Xiaoqian, *J. Phys. Chem. A*, 2006, **110**, 9775.
73 F. Endres and S. Z. Abedinw, *Phys. Chem. Chem. Phys.*, 2006, **8**, 2101.
74 P. Kuhn, A. Forget, D. Su, A. Thomas and M. Antonietti, *J. Am. Chem. Soc.*, 2008, **130**, 13333.
75 J. S. Lee, X. Wang, H. Luo, G. A. Baker and S. Dai, *J. Am. Chem. Soc.*, 2009, **131**, 4596.
76 E. Irran, B. J. Jürgens and W. Schnick, *Chem.–Eur. J.*, 2001, **7**, 5372.
77 W. Schnick, *J. Am. Chem. Soc.*, 2003, **125**, 10288.
78 M. H. Keshavarz and H. R. Pouretedal, *J. Hazard. Mater.*, 2005, **A124**, 27.
79 Test methods according to the UN Recommendations on the Transport of Dangerous Goods, Test 3, 3rd edn, United Nations, New York and Geneva, 1999.
80 ASTM Method D 2540-70, Standard Method for Drop-Weight Sensitivity of Liquid Monopropellants, American Society for Testing and Materials: Philadelphia, PA.
81 Data Bulletin # 61770: Technoproducts Drop-Weight Tester Procedure for Testing Solids, Technoproducts, Inc., Saratoga, CA.
82 G. M. Sheldrick, *SHELXTL version 5.05*, Siemens Analytical X-ray Instruments, Inc., 1996.
83 G. M. Sheldrick, *Program for Semiempirical Absorption Correction of Area Detector Data*, University of Göttingen, Germany, 1996.
84 D. R. MacFarlane, S. A. Forsyth, J. Golding and G. B. Deacon, *Green Chem.*, 2002, **4**, 444.